



FACULTY OF MATHEMATICS,
PHYSICS AND INFORMATICS
Comenius University
Bratislava

TESLA TECHNOLOGY
TTC
COLLABORATION

TTC 2022, TESLA Technology Collaboration

Jan 25 – 27, 2022

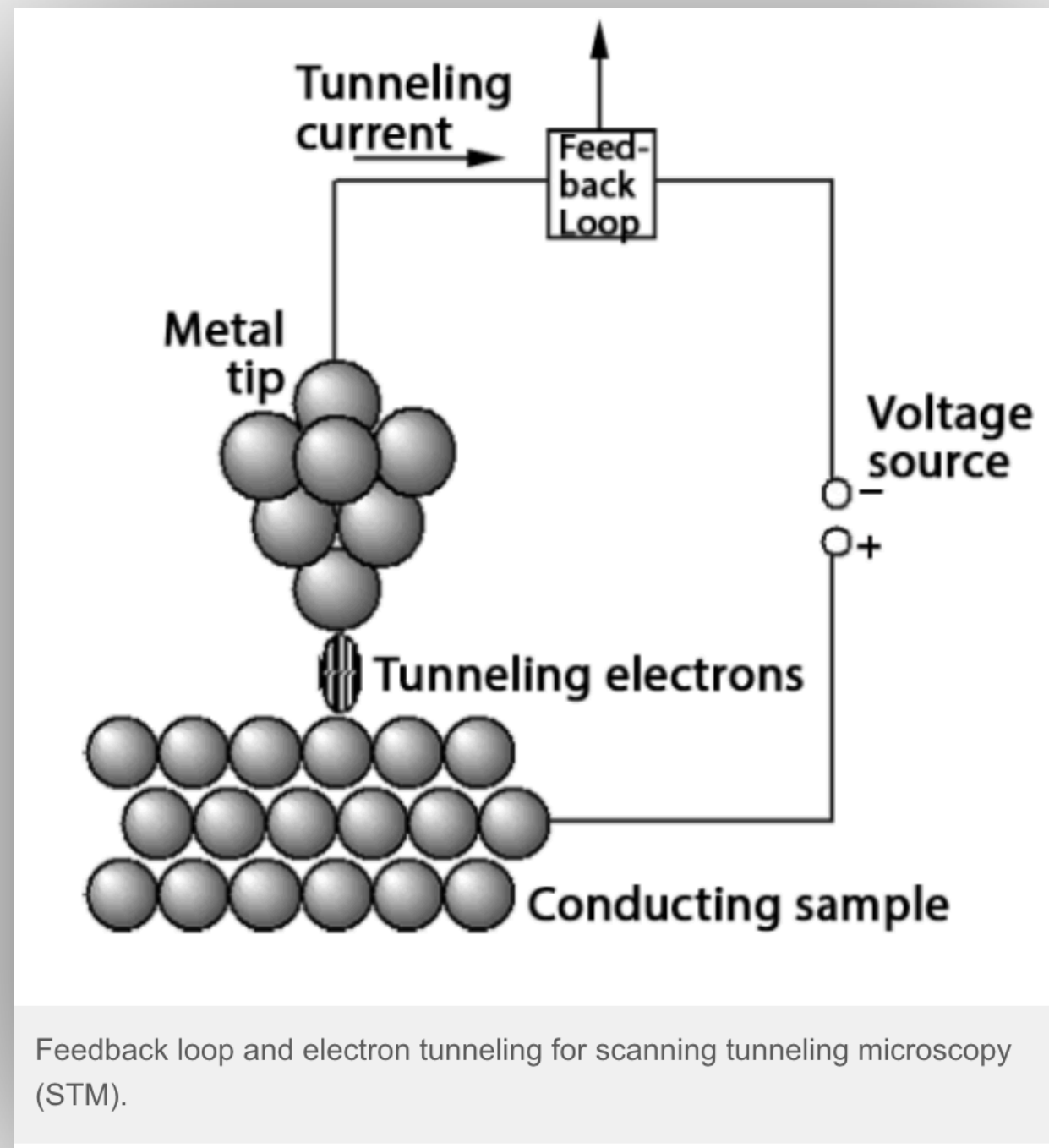
Dynes Superconductors —Implications towards— Radio-Frequency Cavities

The effect of disorder in real-life superconductive samples experiments

František Herman

Dynes Superconductor

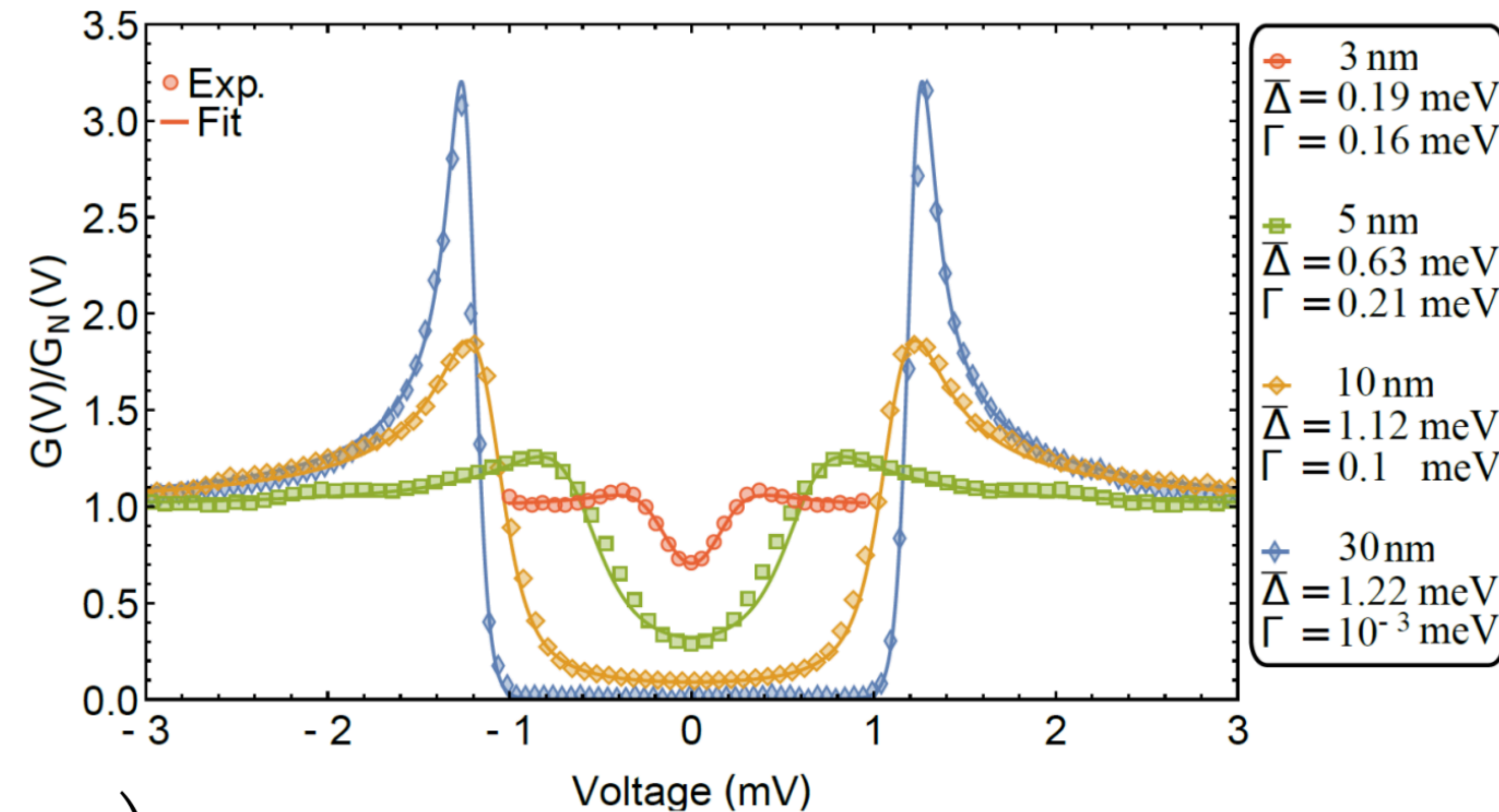
Original motivation



- *Fits to Dynes formula*
- $\bar{\Delta} \gtrsim \Gamma$
- Γ does not vanish at low temperature (*elastic processes*)
- frequently observed (*generic mechanism*)

$$N(\omega) = N_0 \text{Re} \left(\frac{\omega + i\Gamma}{\sqrt{(\omega + i\Gamma)^2 - \Delta^2}} \right)$$

Tunneling conductance of MoC films, $T \approx 0.5\text{K}$



Szabó et al., PRB **93**, 014505 (2016)

Green Function method

In the superconductive state

$$G_R(\mathbf{k}, t - t') = -i\langle\{c_{\mathbf{k}}(t)c_{\mathbf{k}}^+(t')\}\rangle\Theta(t - t')$$

$$\langle X \rangle = Tr \left(X \frac{e^{-H/T}}{Z} \right)$$

$$G(k, \omega_n) = \frac{1}{i\omega_n - \varepsilon_{\mathbf{k}}}$$

$$G(\mathbf{k}, \tau) = \begin{pmatrix} -\langle T c_{\mathbf{k}\uparrow}(\tau) c_{\mathbf{k}\uparrow}^\dagger \rangle & -\langle T c_{\mathbf{k}\uparrow}(\tau) c_{-\mathbf{k}\downarrow} \rangle \\ -\langle T c_{-\mathbf{k}\downarrow}^\dagger(\tau) c_{\mathbf{k}\uparrow}^\dagger \rangle & -\langle T c_{-\mathbf{k}\downarrow}^\dagger(\tau) c_{-\mathbf{k}\downarrow} \rangle \end{pmatrix}$$

Green Function method

In the superconductive state

$$G_R(\mathbf{k}, t - t') = -i\langle\{c_{\mathbf{k}}(t)c_{\mathbf{k}}^+(t')\}\rangle\Theta(t - t')$$

$$\langle X \rangle = Tr \left(X \frac{e^{-H/T}}{Z} \right)$$

$$G(k, \omega_n) = \frac{1}{i\omega_n - \varepsilon_{\mathbf{k}}}$$

$$G(\mathbf{k}, \tau) = \begin{pmatrix} -\langle T c_{\mathbf{k}\uparrow}(\tau) c_{\mathbf{k}\uparrow}^\dagger \rangle & -\langle T c_{\mathbf{k}\uparrow}(\tau) c_{-\mathbf{k}\downarrow} \rangle \\ -\langle T c_{-\mathbf{k}\downarrow}^\dagger(\tau) c_{\mathbf{k}\uparrow}^\dagger \rangle & -\langle T c_{-\mathbf{k}\downarrow}^\dagger(\tau) c_{-\mathbf{k}\downarrow} \rangle \end{pmatrix}$$

- Main object: *Nambu-Gorkov averaged Green's function* \hat{G}_M , defined by: $\hat{G}_M^{-1} = \hat{G}_0^{-1} - \hat{\Sigma}$.

- i) $\hat{G}_0^{-1}(\mathbf{k}, \omega_n) = i\omega_n\tau_0 - \varepsilon_{\mathbf{k}}\tau_3$: the bare Green's function.

ω_n : Matsubara frequencies, τ_i : Pauli matrices.

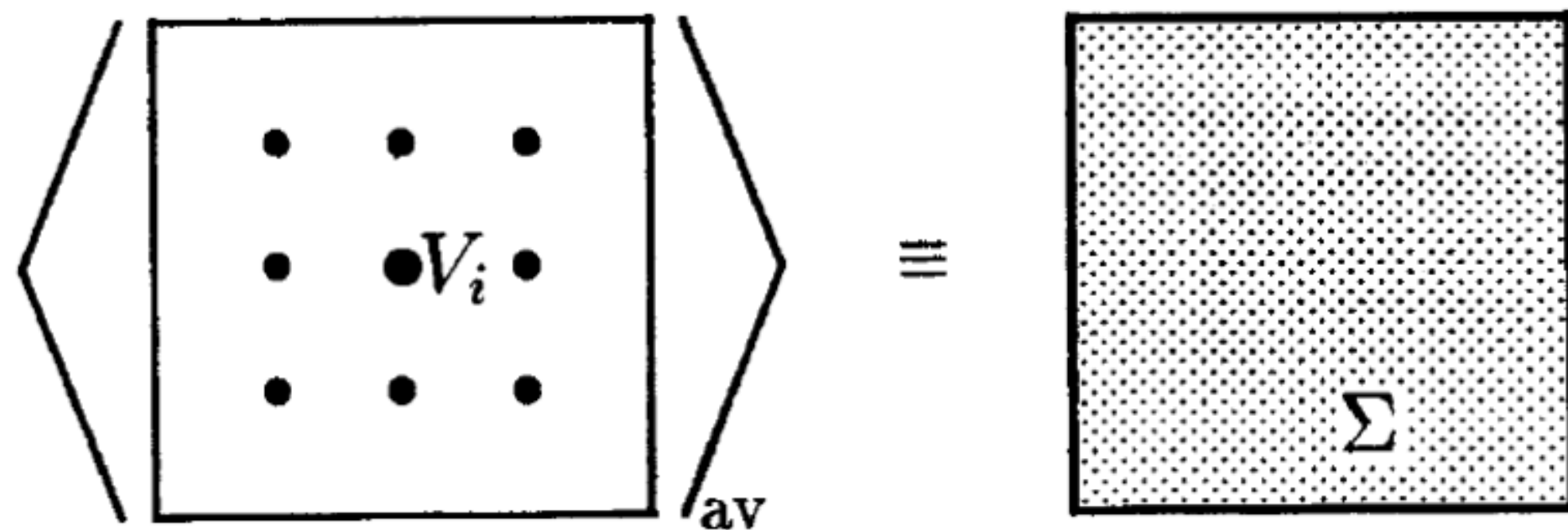
- ii) $\hat{\Sigma}_n = i\omega_n(1 - Z_n)\tau_0 + Z_n\Delta_n\tau_1$: *Self-energy* generated by disorder and pairing interactions. Functions Δ_n and Z_n contain complete information about the properties of the considered superconductor.

Coherent Potential Approximation

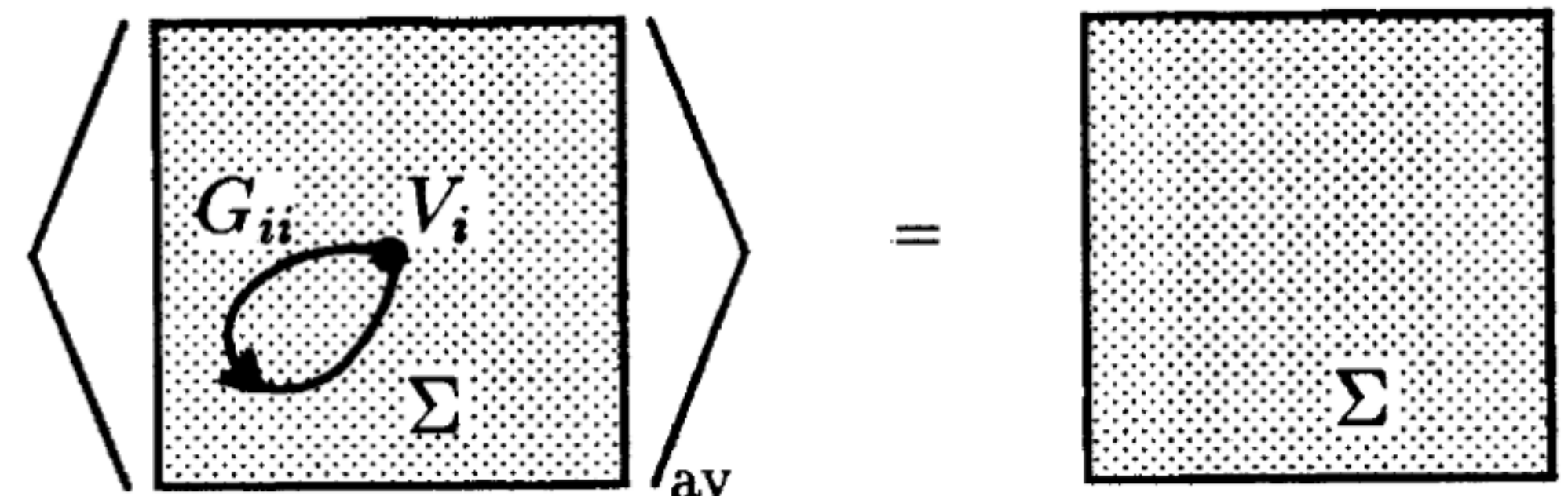
Soven, Velický et. al., Weinkauff and Zittart 75

CPA (*nonperturbative approach* \rightarrow *self-consistent theory*):

(a)

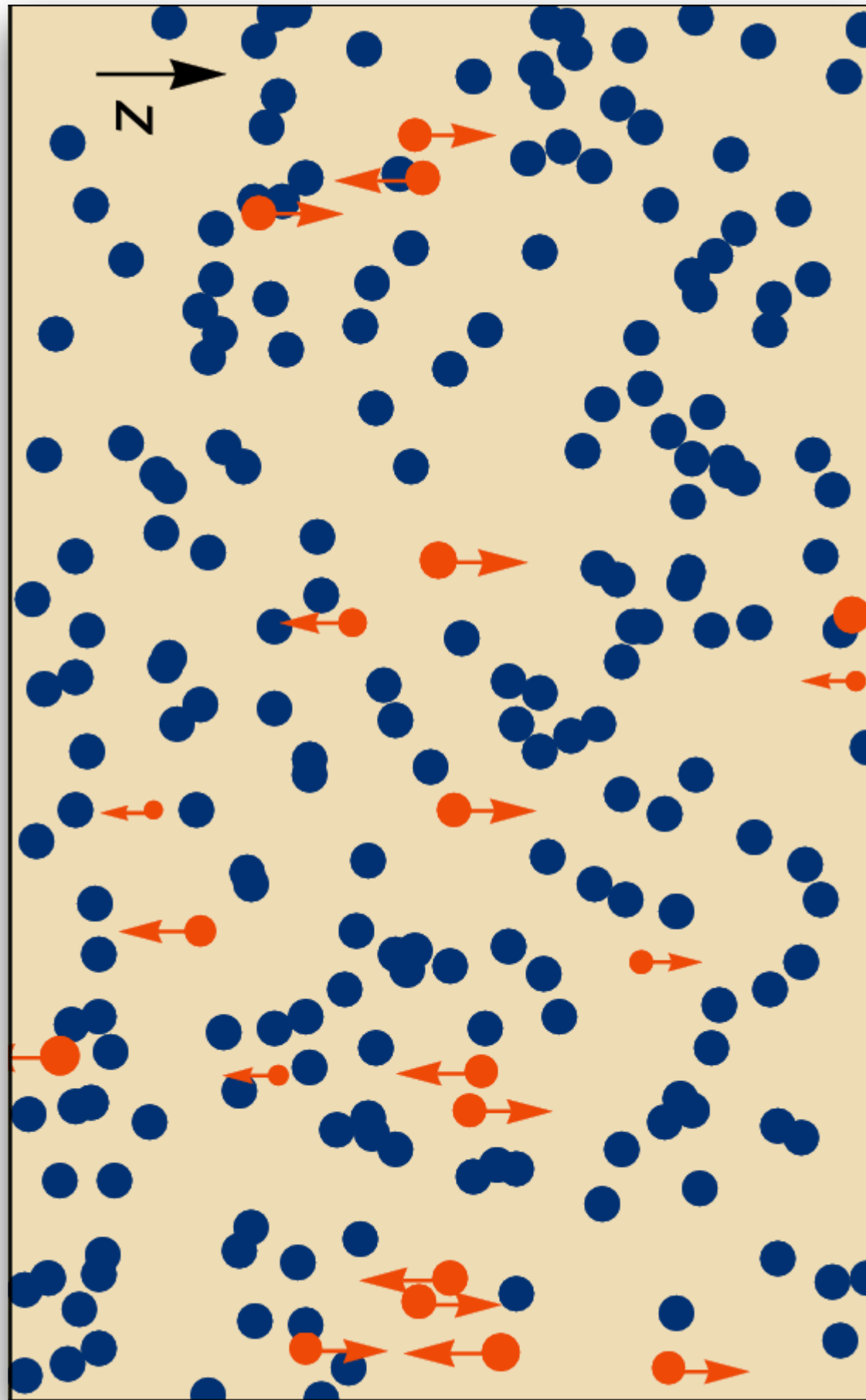


(b)



$$\hat{\mathcal{G}}_n = \frac{1}{\mathcal{N}} \sum_{\mathbf{k}} \hat{G}(n\mathbf{k}), \quad \hat{\mathcal{G}}_n = \left\langle \left(\hat{\mathcal{G}}_n^{-1} - \hat{V} + \hat{\Sigma}_n \right)^{-1} \right\rangle$$

Dynes Superconductor Model



- Hamiltonian:

$$H = H_0 + \sum_i \bar{\Delta} (c_{i\downarrow} c_{i\uparrow} + h.c.) + \sum_{i,\sigma} (U_i c_{i\sigma}^\dagger c_{i\sigma} + V_i \sigma c_{i\sigma}^\dagger c_{i\sigma})$$

H_0 : free electrons.

$\bar{\Delta}$: spatially homogeneous pairing interaction.

U : pair-conserving fluctuating field.

V : pair-breaking fluctuating field with fixed polarization in spin space.

- $P_s(U)$ and $P_m(V)$: Uncorrelated and even distributions of potential (U) and magnetic (V) impurities.

Green function + CPA

- Main object: *Nambu-Gorkov averaged Green's function*

\hat{G}_M , defined by: $\hat{G}_M^{-1} = \hat{G}_0^{-1} - \hat{\Sigma}$.

- i) $\hat{G}_0^{-1}(\mathbf{k}, \omega_n) = i\omega_n\tau_0 - \varepsilon_{\mathbf{k}}\tau_3$: the bare Green's function.

ω_n : Matsubara frequencies, τ_i : Pauli matrices.

- ii) $\hat{\Sigma}_n = i\omega_n(1 - Z_n)\tau_0 + Z_n\Delta_n\tau_1$: *Self-energy* generated by disorder and pairing interactions. Functions Δ_n and Z_n contain complete information about the properties of the considered superconductor.

- CPA equations:

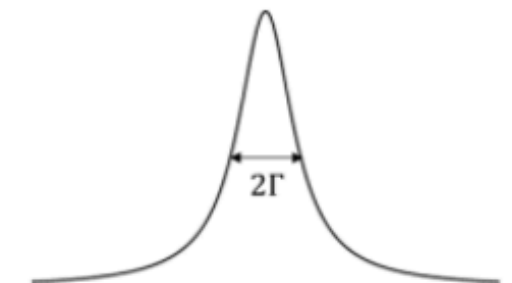
$$\hat{\mathcal{G}}_n = \left\langle \left(\hat{\mathcal{G}}_n^{-1} - \hat{V} + \hat{\Sigma}_n \right)^{-1} \right\rangle$$

Impurity potential: $\hat{V} = \bar{\Delta}\tau_1 + U\tau_3 + V\tau_0$.

The index *ii* denotes the diagonal component (in coordinate space) of a matrix and

$$\langle f(U, V) \rangle = \int dU \int dV P_s(U) P_m(V) f(U, V).$$

$$CPA + \left\{ \begin{array}{l} P_s(U) : \\ \text{arbitrary} \end{array} \right\} + \left\{ \begin{array}{l} P_m(V) : \text{Lorentzian} \\ \text{Diagram} \end{array} \right\}$$



Dynes Superconductor

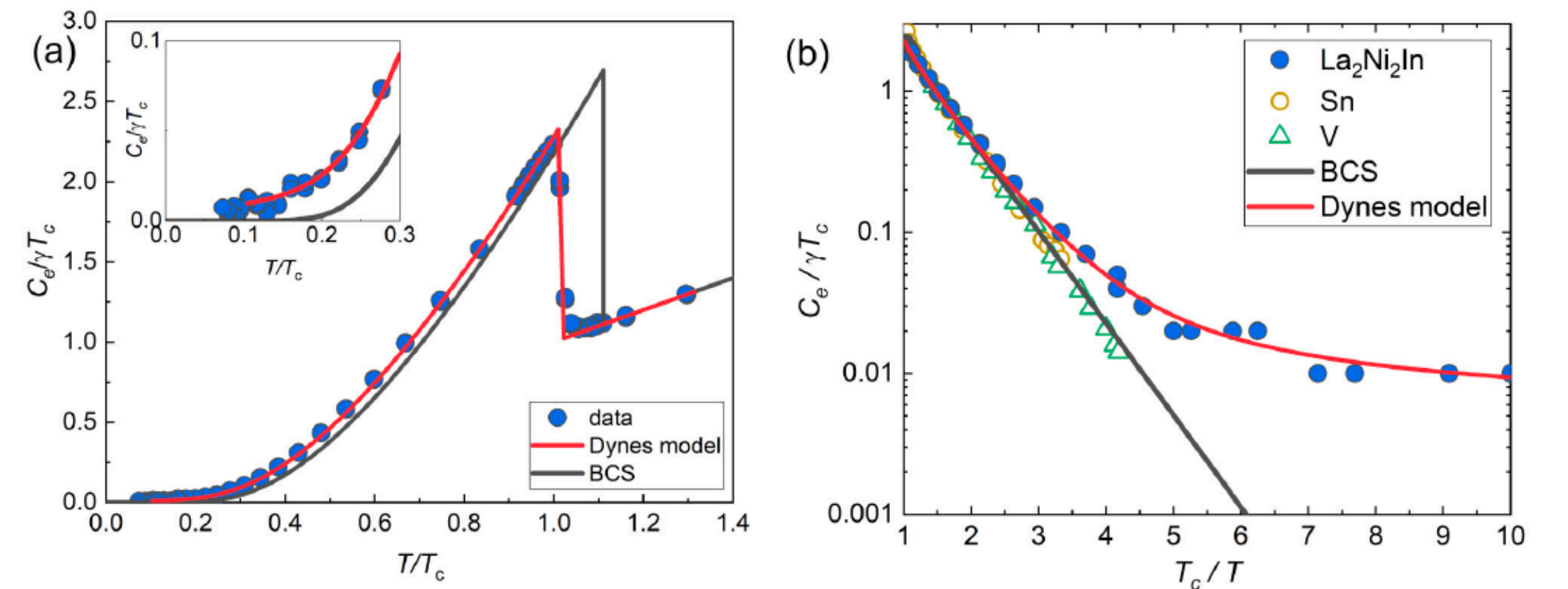
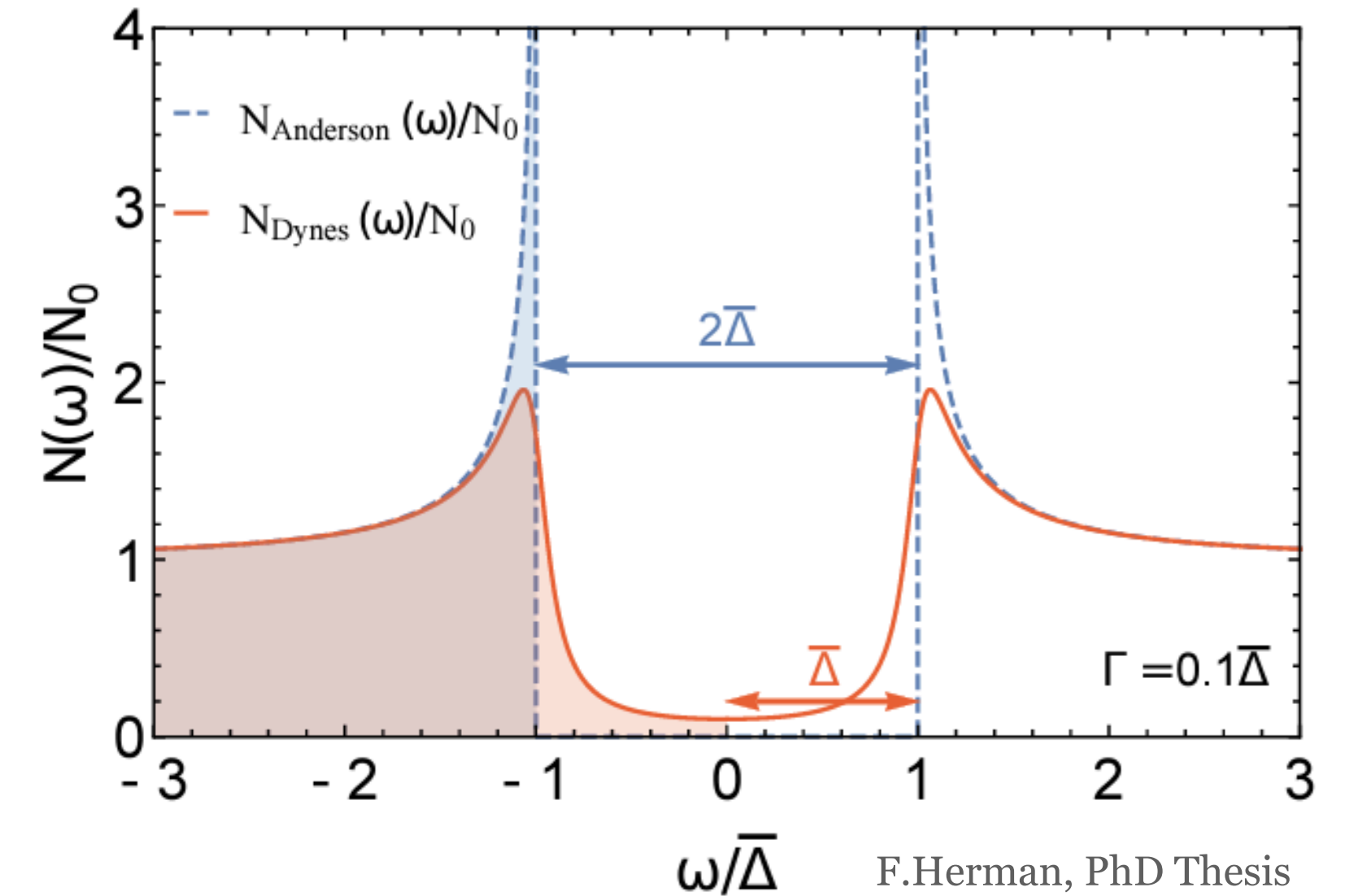
From the bullet train

- Generalization of the BCS superconductor including pair-breaking and pair-conserving scattering processes (smearing of all undesired infinities)
- Mathematical formulation using Green function method:

$$\hat{G}(\mathbf{k}, \omega) = \frac{1}{2} \delta \ln [\epsilon_{\mathbf{k}}^2 - \epsilon(\omega)^2],$$

$$\delta = \tau_0 \partial_{\omega} - \tau_1 \partial_{\Delta} - \tau_3 \partial_{\epsilon_{\mathbf{k}}},$$

$$\epsilon(\omega) = \sqrt{(\omega + i\Gamma)^2 - \Delta^2} + i\Gamma_s.$$



Dynes Superconductor Generalization

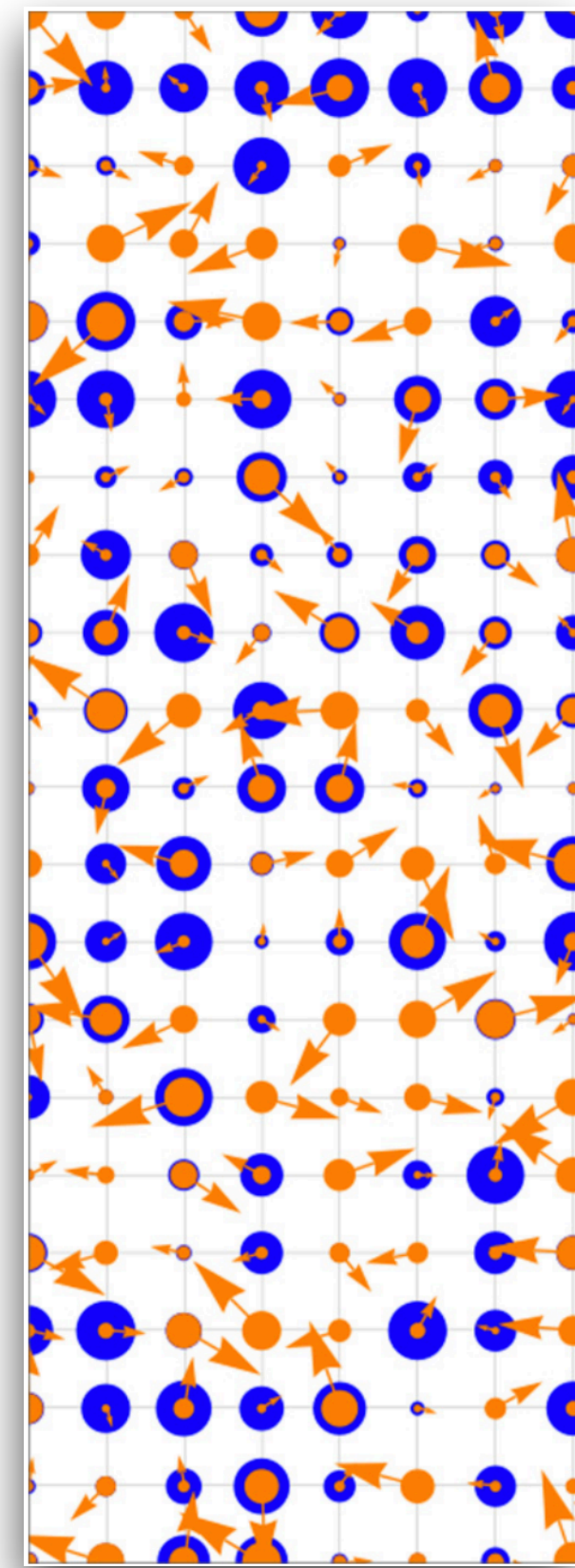
From the bullet train

- Generalization of the BCS superconductor including pair-breaking and pair-conserving scattering processes (smearing of all undesired infinities)
- Mathematical formulation using Green function method:

$$\hat{G}(\mathbf{k}, \omega) = \frac{1}{2} \delta \ln [\epsilon_{\mathbf{k}}^2 - \epsilon(\omega)^2],$$

$$\delta = \gamma_0 \partial_{\omega} - \gamma_1 \partial_{\Delta} - \gamma_3 \partial_{\epsilon_{\mathbf{k}}},$$

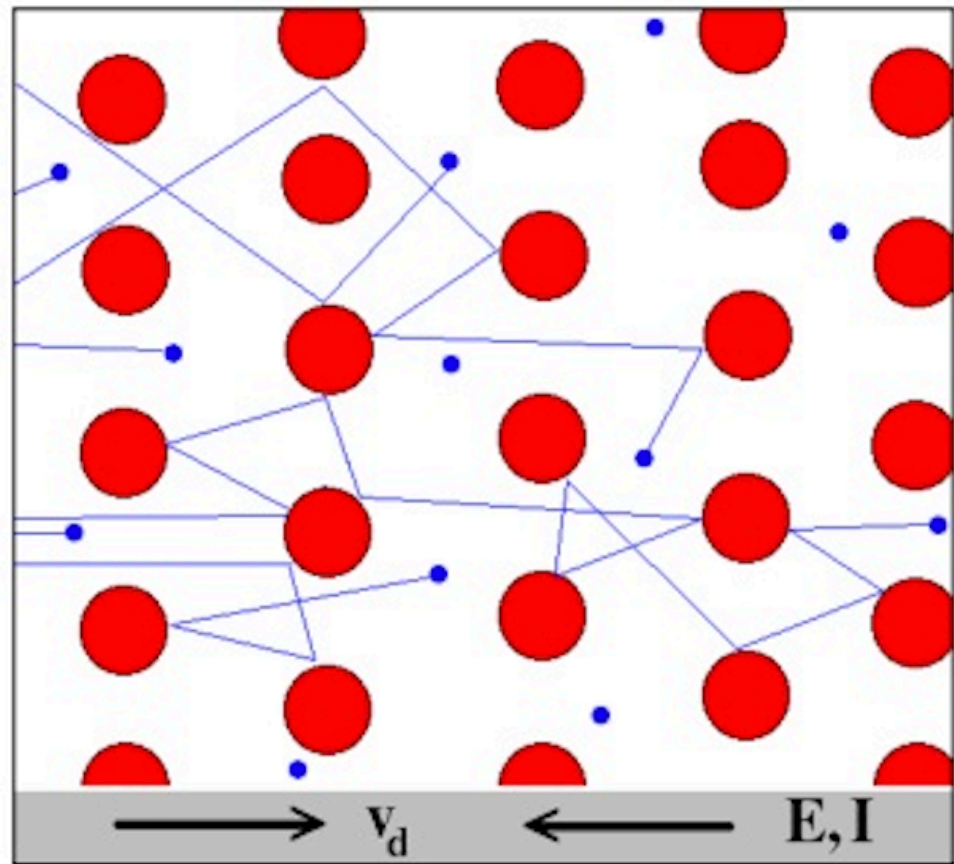
$$\epsilon(\omega) = \sqrt{(\omega + i\Gamma)^2 - \Delta^2} + i\Gamma_s.$$



Dynes Superconductor

Electromagnetic properties and optical conductivity

Drude Model



Paul Karl Ludwig Drude (1863–1906)

The electron moves at the Fermi speed, and has only a tiny drift velocity superimposed by the applied electric field.

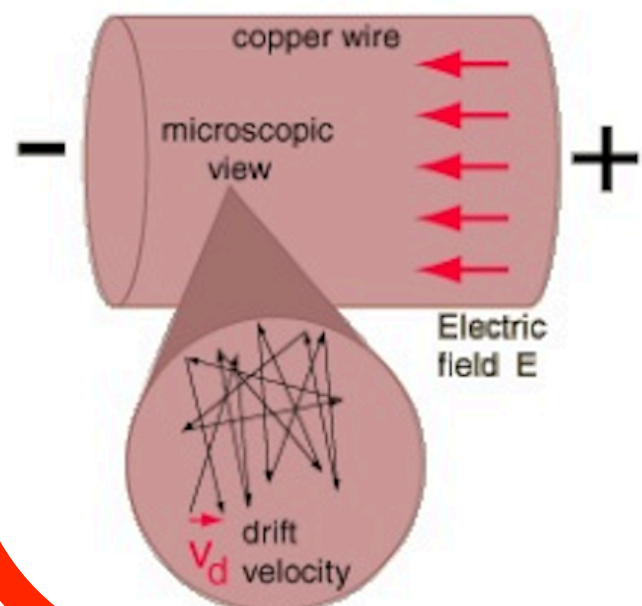
$$\vec{p} = m_e \vec{v} = e \vec{E} \tau$$

$$\vec{J} = ne\vec{v}$$



drift velocity

$$\vec{J} = \left(\frac{ne^2\tau}{m_e} \right) \vec{E}$$

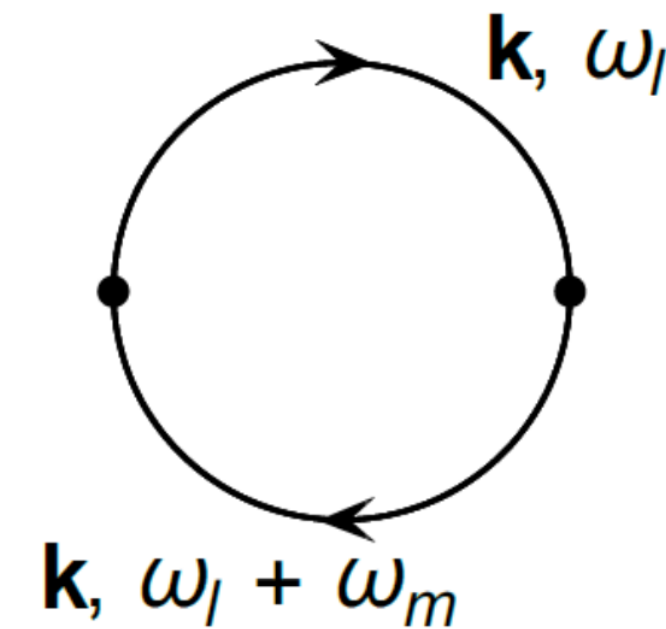


Electromagnetic properties of impure superconductors with pair-breaking processes

František Herman and Richard Hlubina

Phys. Rev. B **96**, 014509 – Published 12 July 2017

$$\sigma(\omega) = \frac{i}{\omega + i0^+} K(\omega),$$



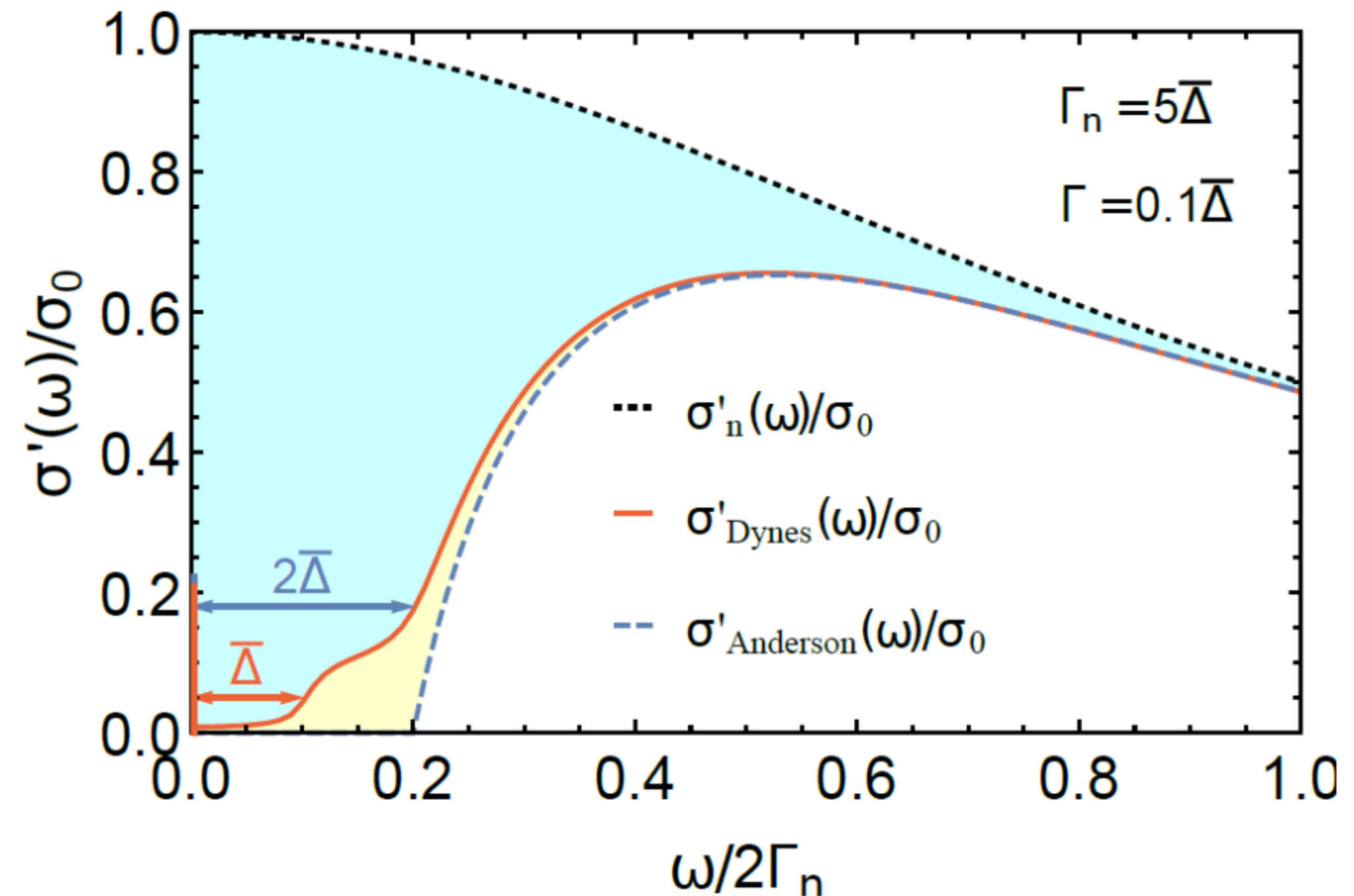
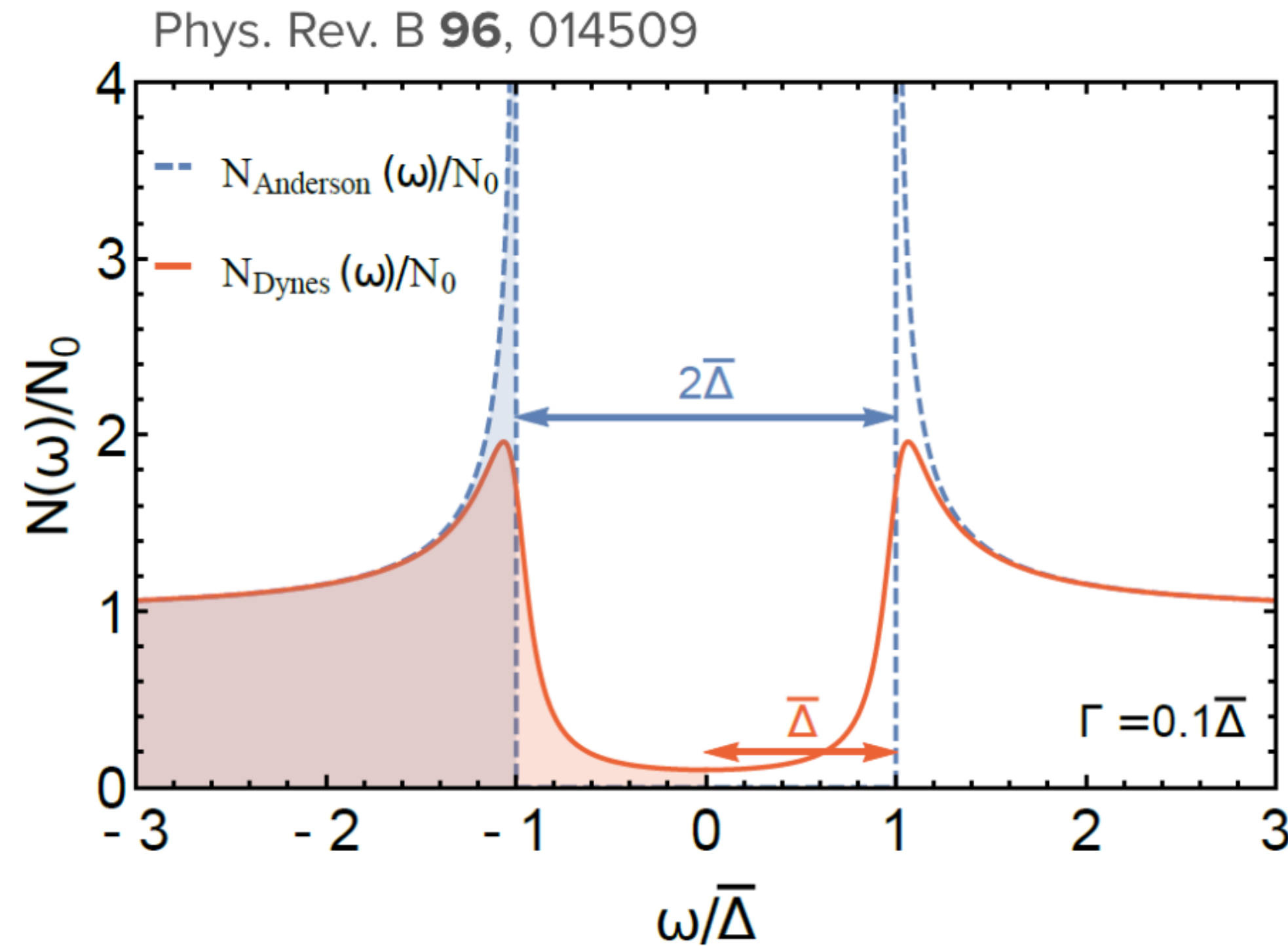
$$K(\omega_m) = D_0 + \frac{e^2 v_F^2}{3} \int \frac{d^3 \mathbf{k}}{(2\pi)^3} T \sum_{\omega_l} \text{Tr} \left[\hat{G}(\mathbf{k}, \omega_l + \omega_m) \hat{G}(\mathbf{k}, \omega_l) \right]$$

diamagnetic part

paramagnetic part

Dynes Superconductor

Electromagnetic properties and optical conductivity



→ Optical Conductivity: $\sigma(\omega) = \pi D \delta(\omega) + \sigma_{\text{reg}}(\omega)$

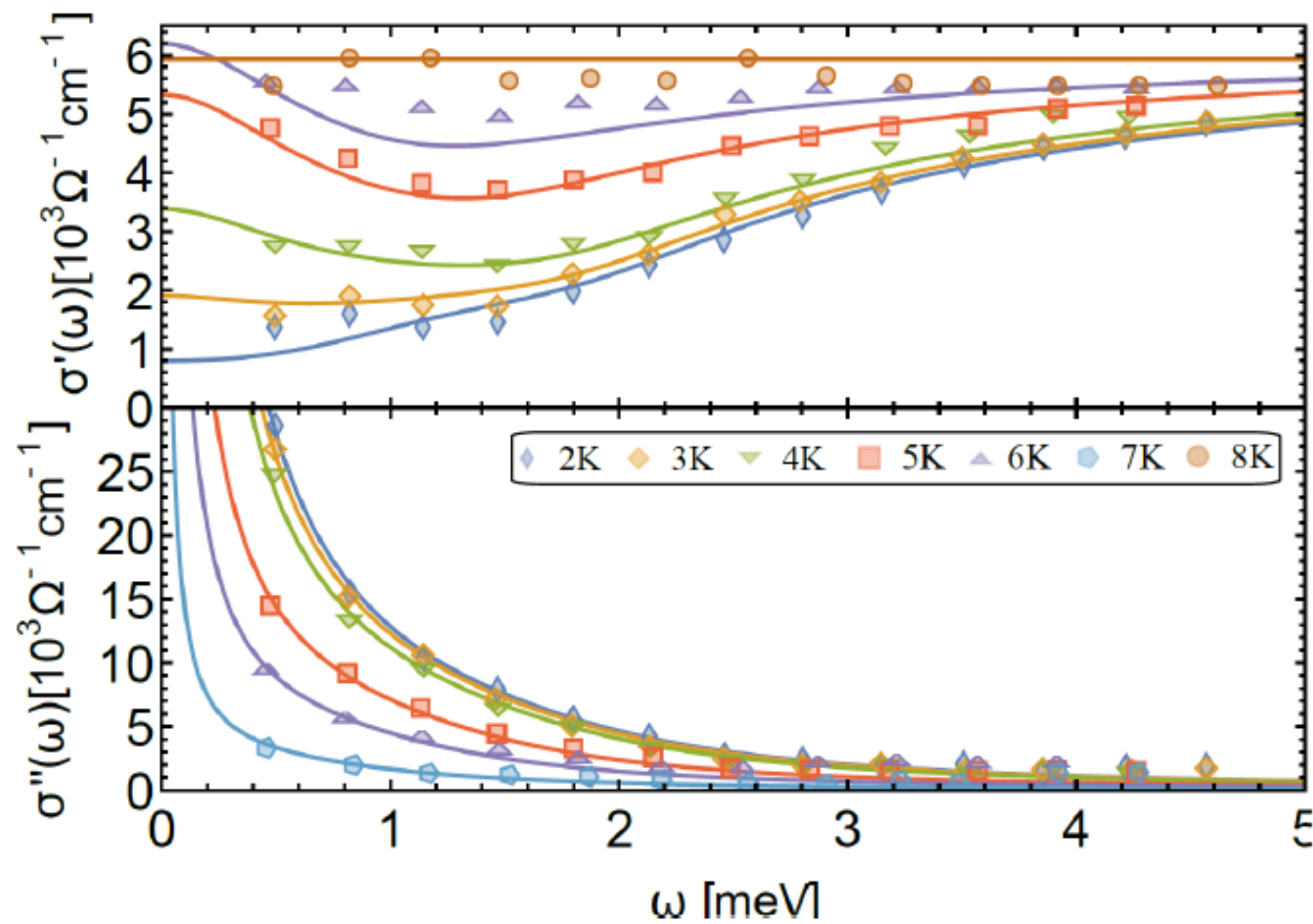
→ Two absorption edges at $\omega = \bar{\Delta}$ and $\omega = 2\bar{\Delta}$

→ sum rule: $\int_0^\infty d\omega \sigma'(\omega) = \pi/2$

→ $\sigma'_{\text{reg}}(\omega)$ finite down to $\omega \rightarrow 0$ and $T \rightarrow 0$

Dynes Superconductor

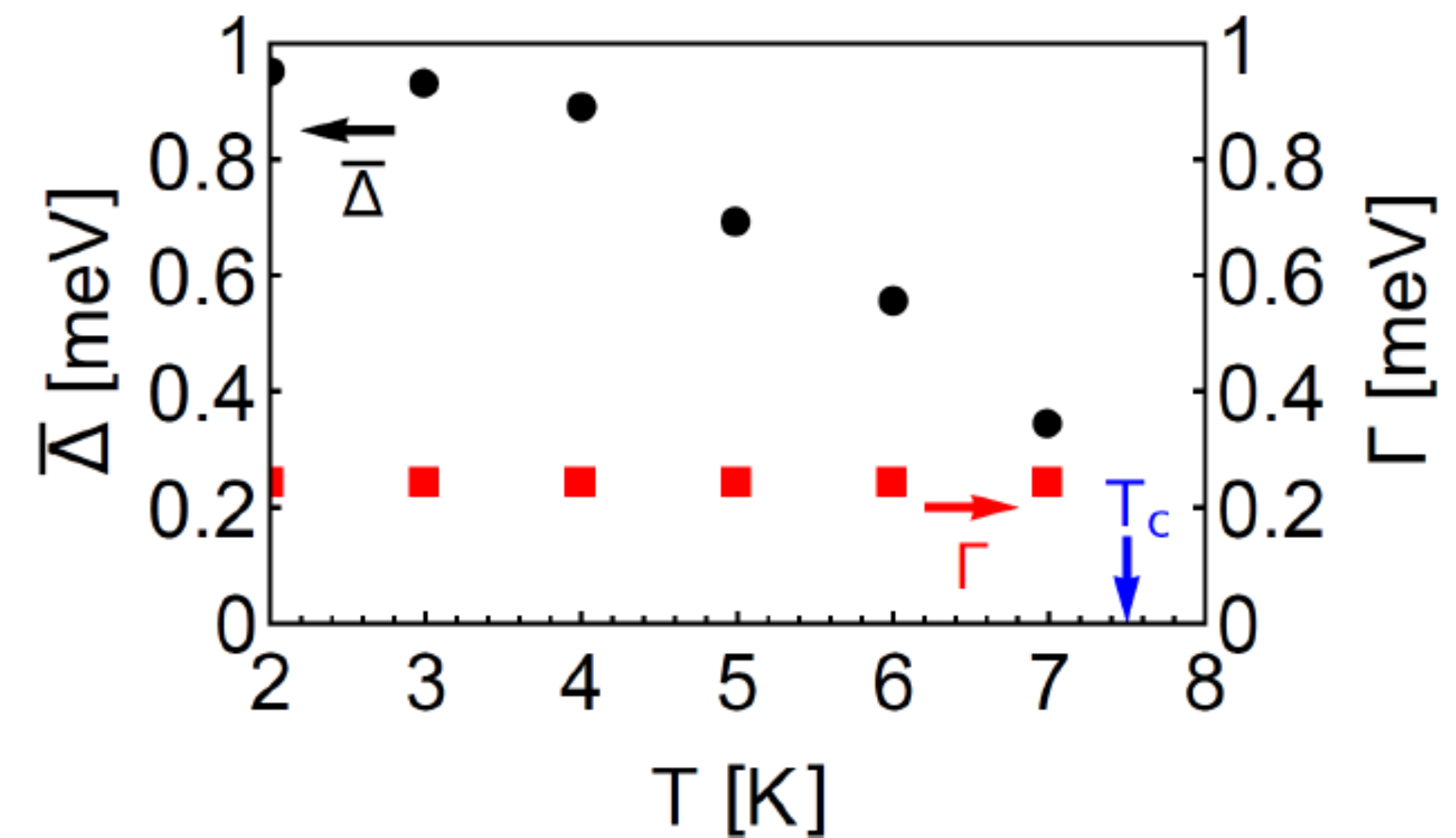
Electromagnetic properties and optical conductivity



J. Simmendinger *et al.*, PRB **94**, 064506 (2016)

→ $T = 2\text{K}$: 3 parameters $\{\sigma_0, \bar{\Delta}(T), \Gamma\}$

→ $T > 2\text{K}$: 1 parameter $\{\bar{\Delta}(T)\}$



Phys. Rev. B **96**, 014509

Dynes Superconductor

Implications towards the superconductive cavities: **Coherence peak**

Microwave response of superconductors that obey local electrodynamics

František Herman and Richard Hlubina

Phys. Rev. B **104**, 094519 – Published 21 September 2021

$$\hbar\omega < \Gamma \ll \Gamma_s \lesssim \Delta_0. \quad (6)$$

In other words, we will be concerned with moderately clean superconductors with weak but non-vanishing pair-breaking scattering.

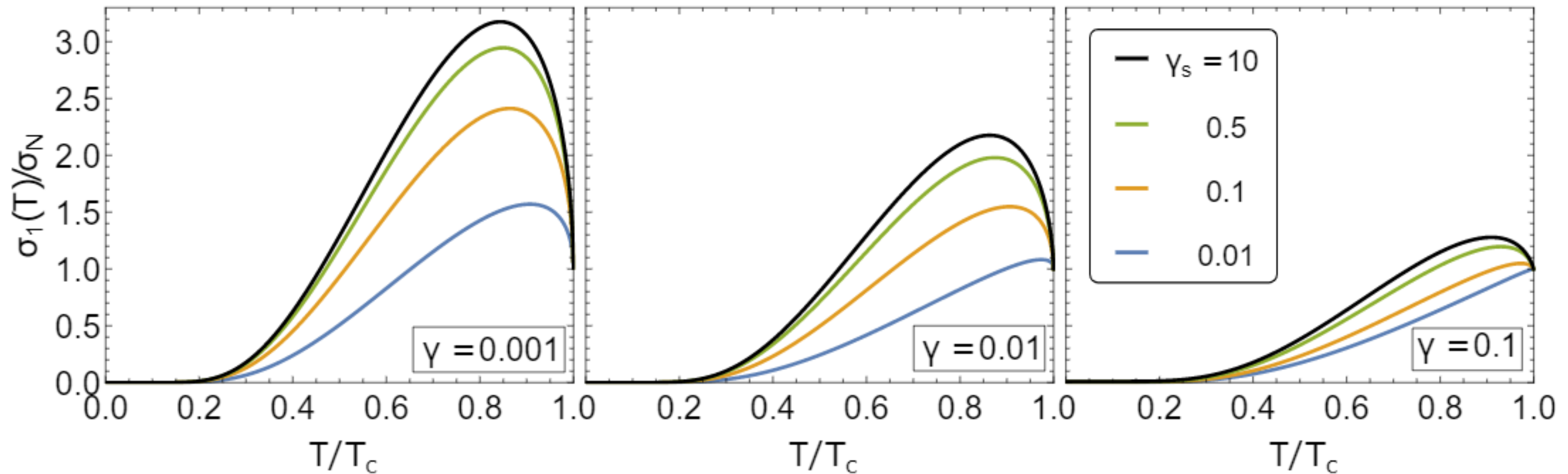


FIG. 1. Temperature dependence of the $\omega \rightarrow 0$ limit of $\sigma_1(T)/\sigma_N$ as a function of T/T_c for several values of γ and γ_s . Note that the same peak height can be reached for different combinations of γ and γ_s .

Dynes Superconductor

Implications towards the superconductive cavities: **Coherence peak**

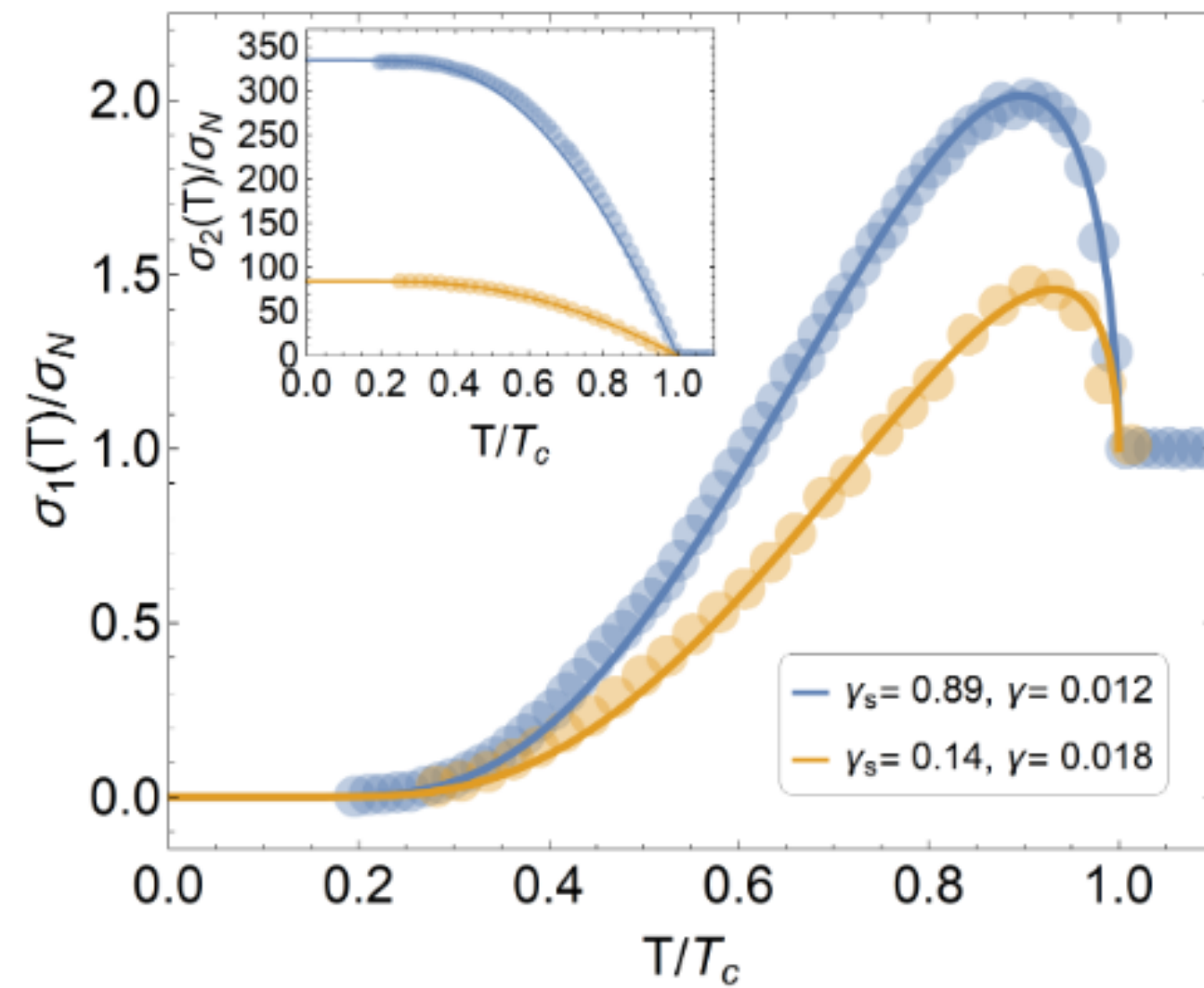


FIG. 9. Real and imaginary parts of the conductivities of the two samples from Fig. 4 in [13] (symbols), together with their fits by the theory of Dynes superconductors with the strong-coupling corrections described for both samples by $x = 1.145$ (lines).

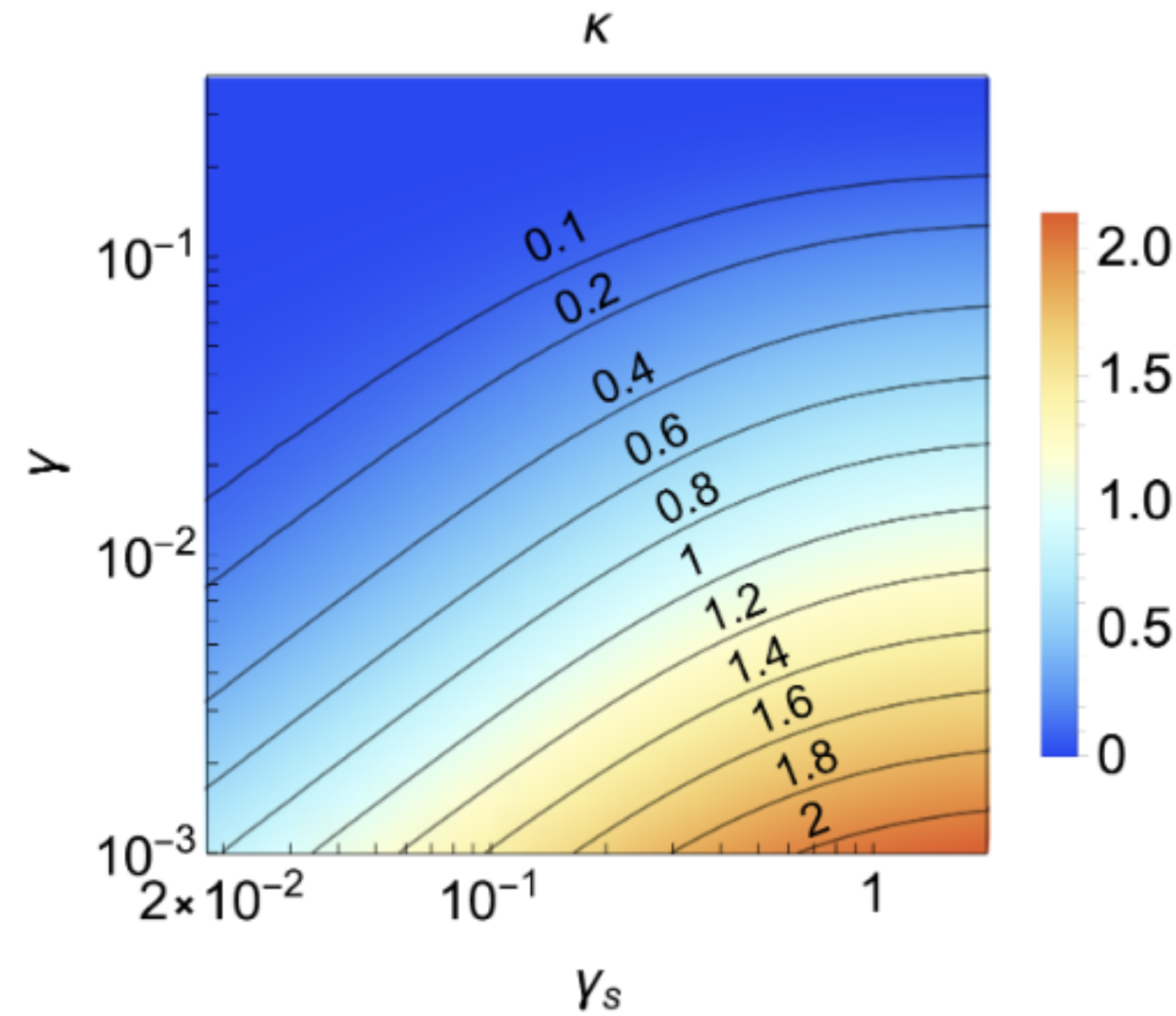


FIG. 2. Height of the coherence peak $\kappa = \sigma_{1,\max}/\sigma_N - 1$ (magnitude indicated by the black labels) as a function of the dimensionless scattering rates γ_s and γ .

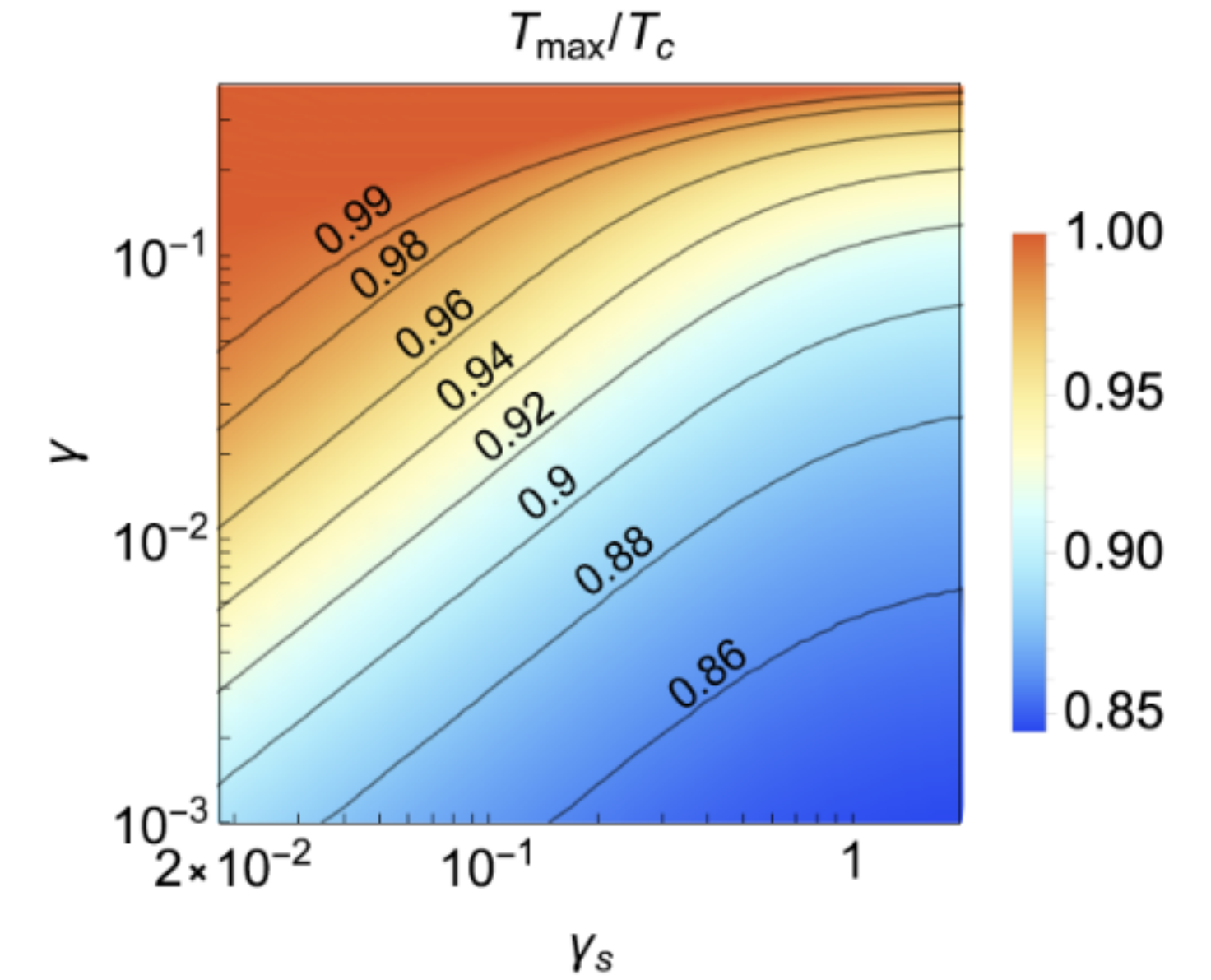


FIG. 4. Position T_{\max}/T_c (indicated by the black labels) of the coherence peak of σ_1/σ_N as a function of γ_s and γ .

Phys. Rev. B **104**, 094519

Dynes Superconductor

Implications towards the superconductive cavities: **Coherence peak**

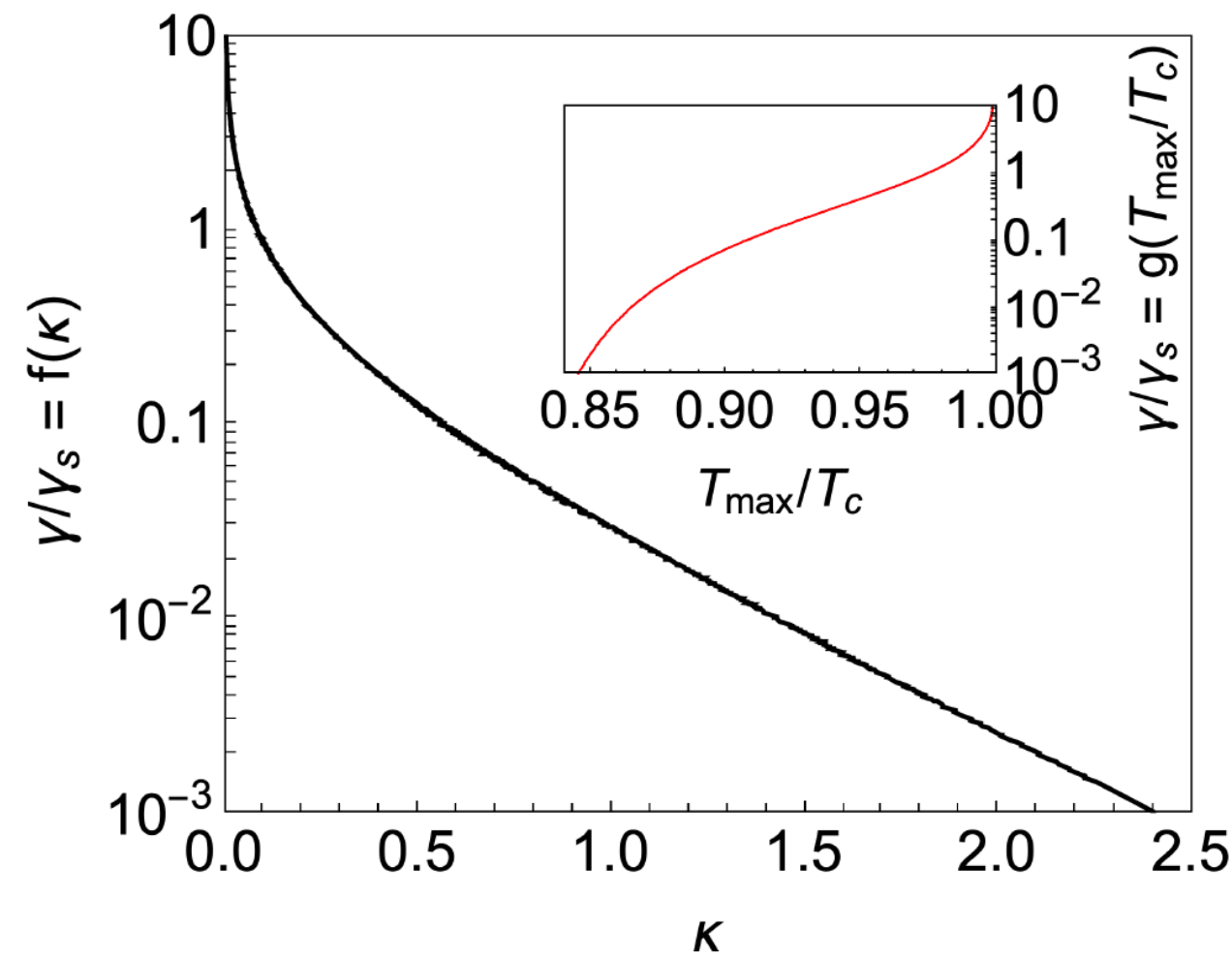


FIG. 3. Dependence of the slopes $\gamma/\gamma_s = f(\kappa)$ of the equal- κ lines in the small-scattering rate corner of Fig. 2 on the coherence-peak height κ . The inset shows an analogous plot of the slopes γ/γ_s of the equal- T_{\max}/T_c lines in the small-scattering rate corner of Fig. 4 as a function of T_{\max}/T_c .

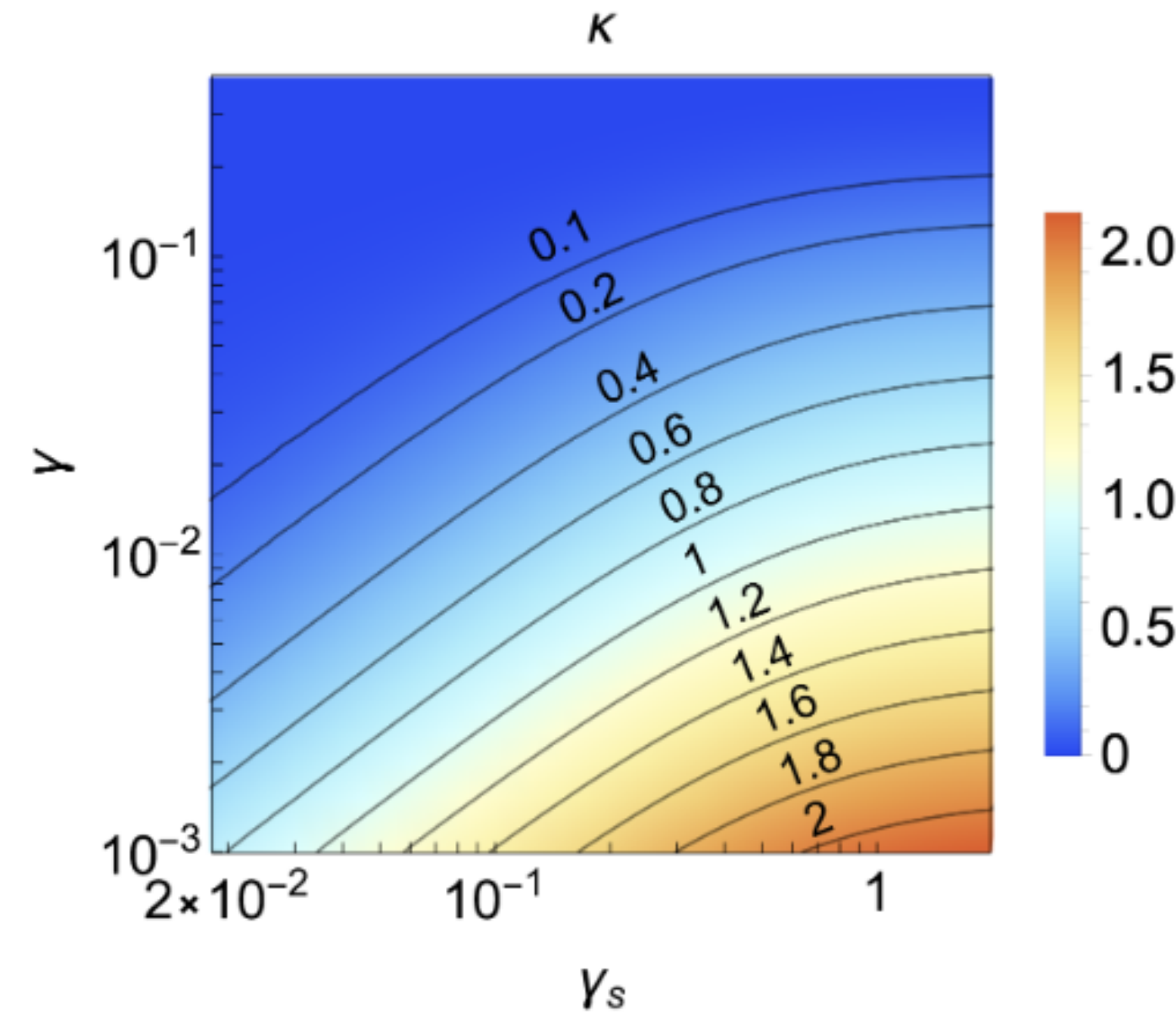


FIG. 2. Height of the coherence peak $\kappa = \sigma_{1,\max}/\sigma_N - 1$ (magnitude indicated by the black labels) as a function of the dimensionless scattering rates γ_s and γ .

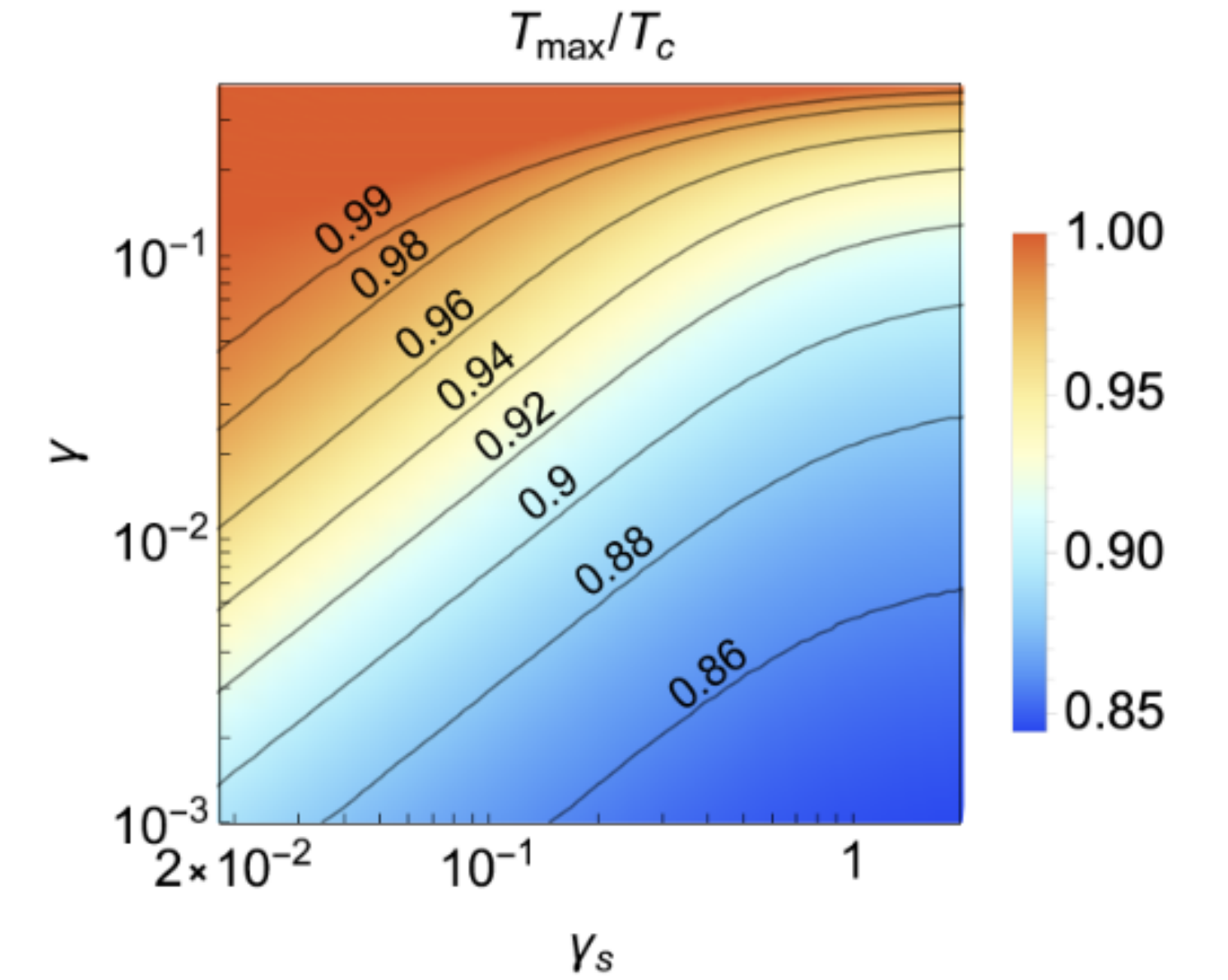


FIG. 4. Position T_{\max}/T_c (indicated by the black labels) of the coherence peak of σ_1/σ_N as a function of γ_s and γ .

Phys. Rev. B **104**, 094519

Dynes Superconductor

Implications towards the superconductive cavities: **Coherence peak**

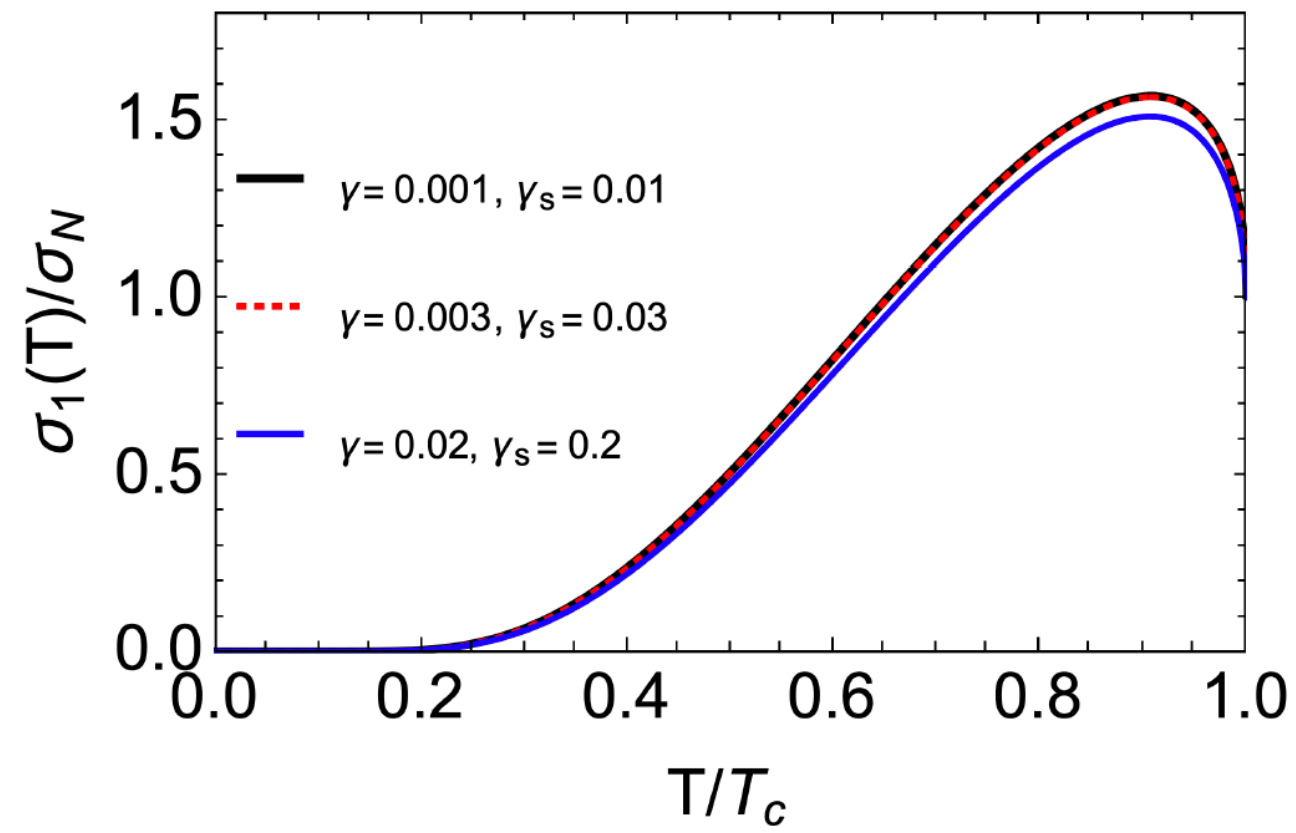


FIG. 5. Temperature dependence of the real part of the microwave conductivity $\sigma_1(T)/\sigma_N$ for three choices of γ and γ_s with a fixed ratio γ/γ_s .

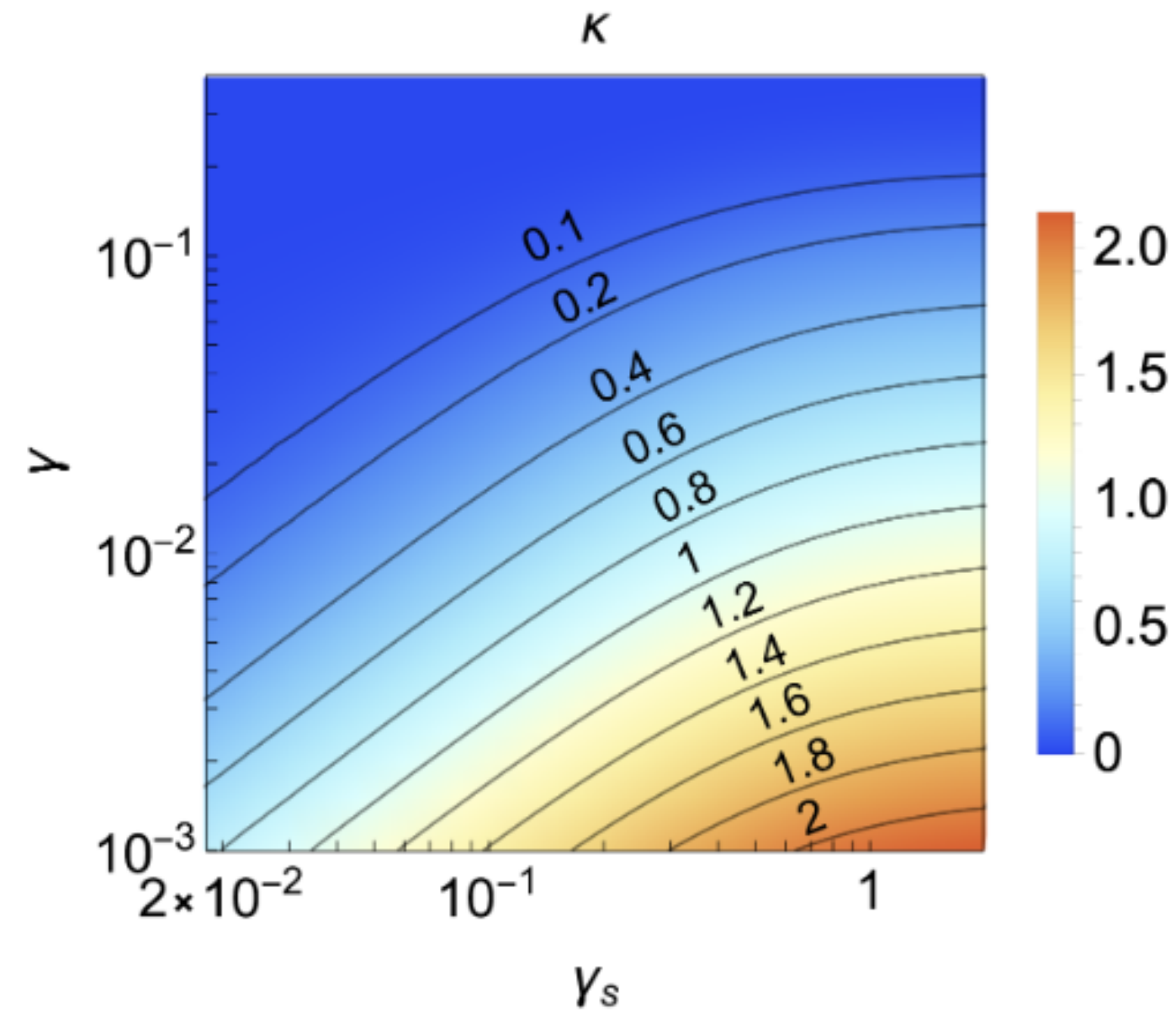


FIG. 2. Height of the coherence peak $\kappa = \sigma_{1,\max}/\sigma_N - 1$ (magnitude indicated by the black labels) as a function of the dimensionless scattering rates γ_s and γ .

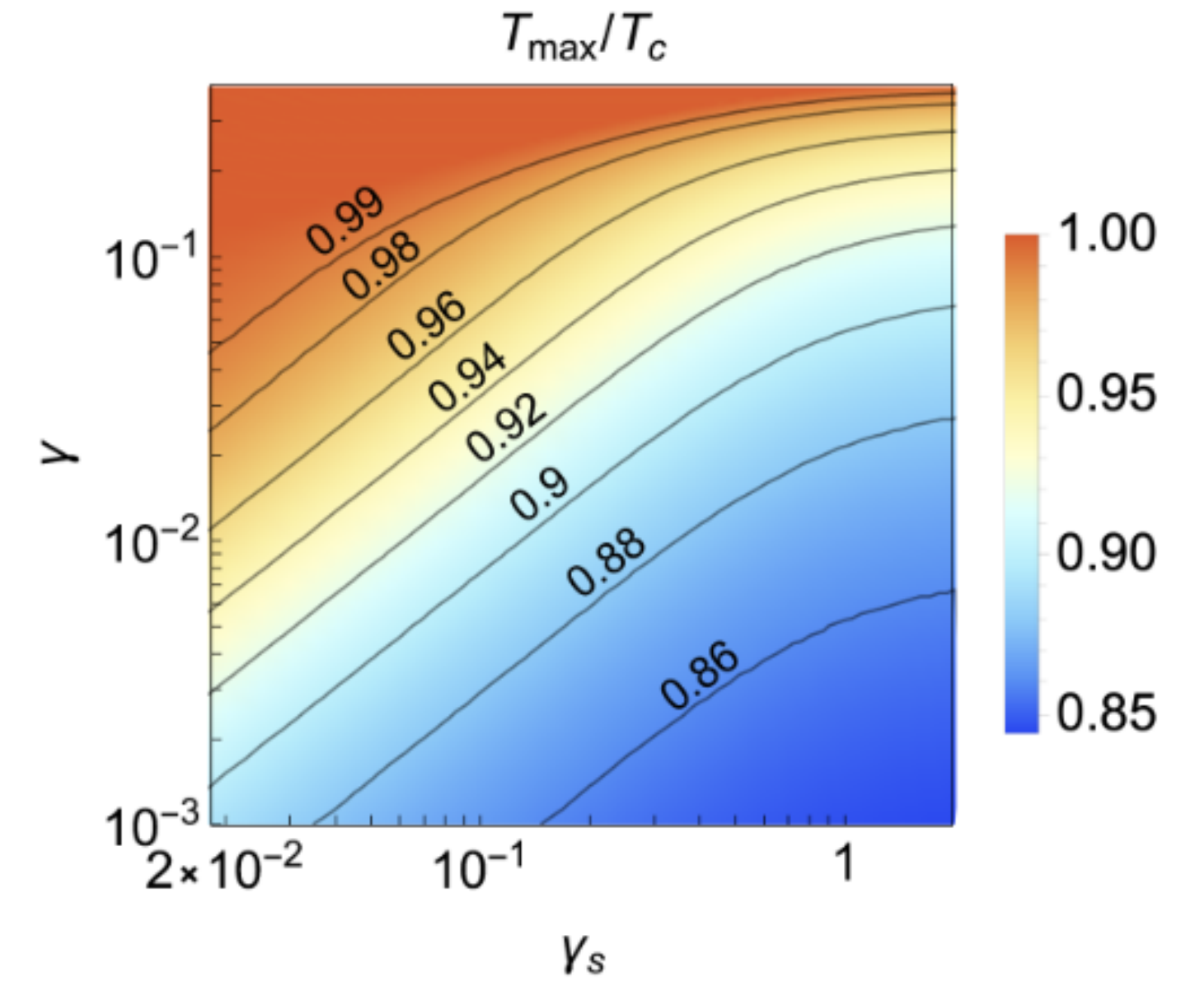


FIG. 4. Position T_{\max}/T_c (indicated by the black labels) of the coherence peak of σ_1/σ_N as a function of γ_s and γ .

Phys. Rev. B **104**, 094519

Dynes Superconductor

Implications towards the superconductive cavities: **Coherence peak** and **Imaginary part of DC Conductivity**

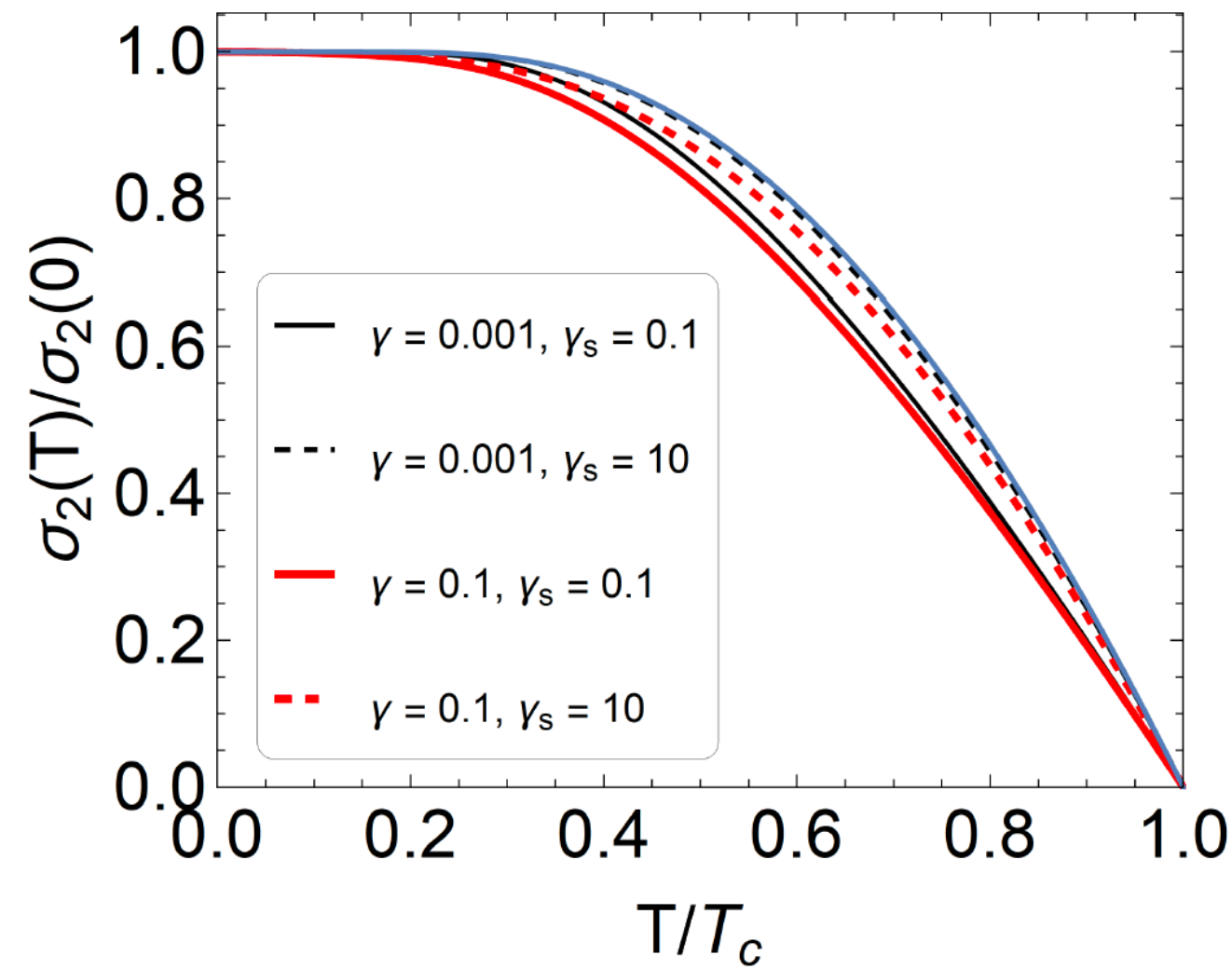


FIG. 6. Temperature dependence of the imaginary part of the microwave conductivity $\sigma_2(T)/\sigma_2(0)$ for several choices of γ and γ_s . Note that when γ_s decreases and γ increases, the curves are pushed slightly downwards with respect to Eq. (14), which is shown by the blue line.

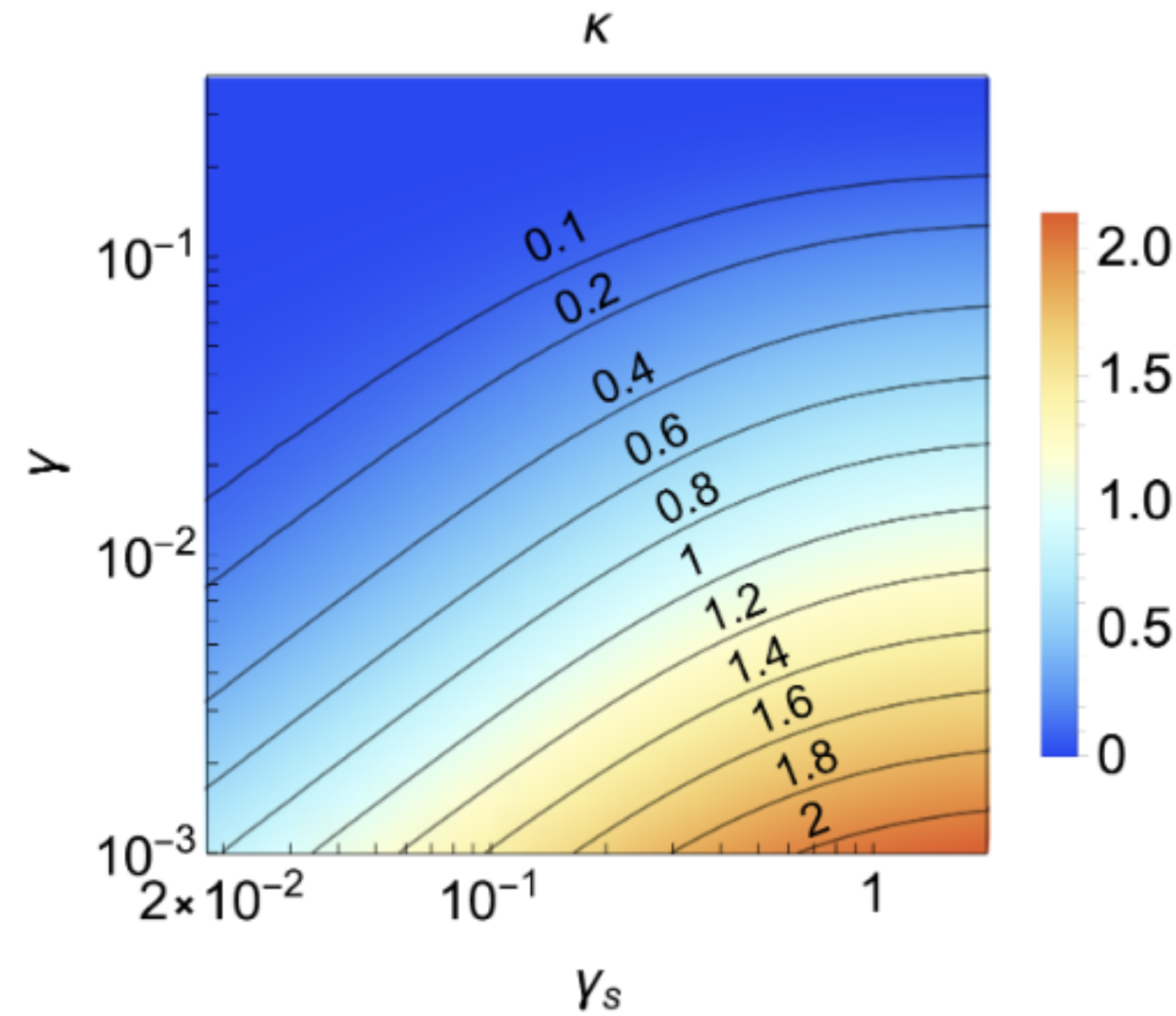


FIG. 2. Height of the coherence peak $\kappa = \sigma_{1,\max}/\sigma_N - 1$ (magnitude indicated by the black labels) as a function of the dimensionless scattering rates γ_s and γ .

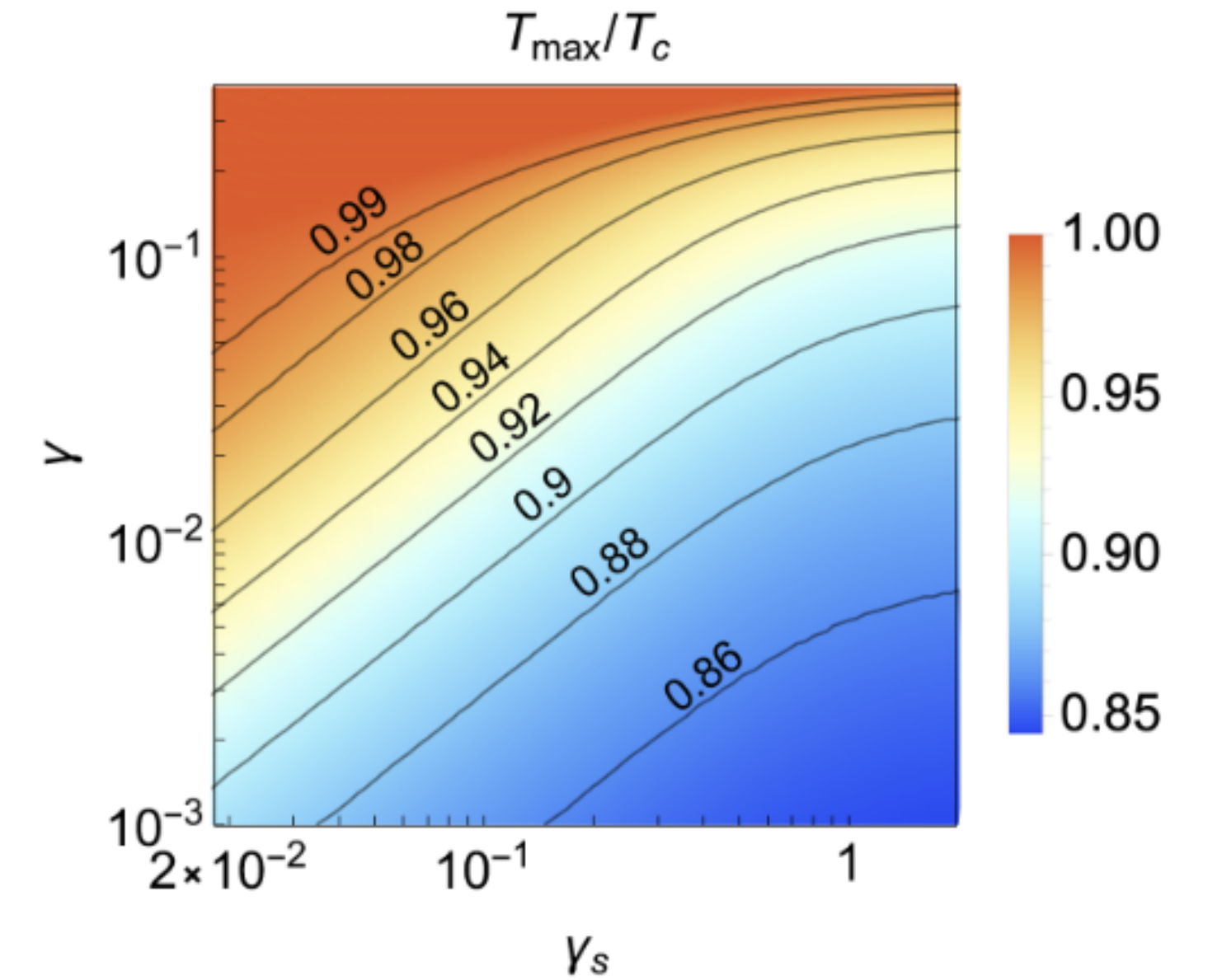


FIG. 4. Position T_{\max}/T_c (indicated by the black labels) of the coherence peak of σ_1/σ_N as a function of γ_s and γ .

Phys. Rev. B **104**, 094519

Dynes Superconductor

Implications towards the superconductive cavities: **Imaginary part of DC Conductivity**

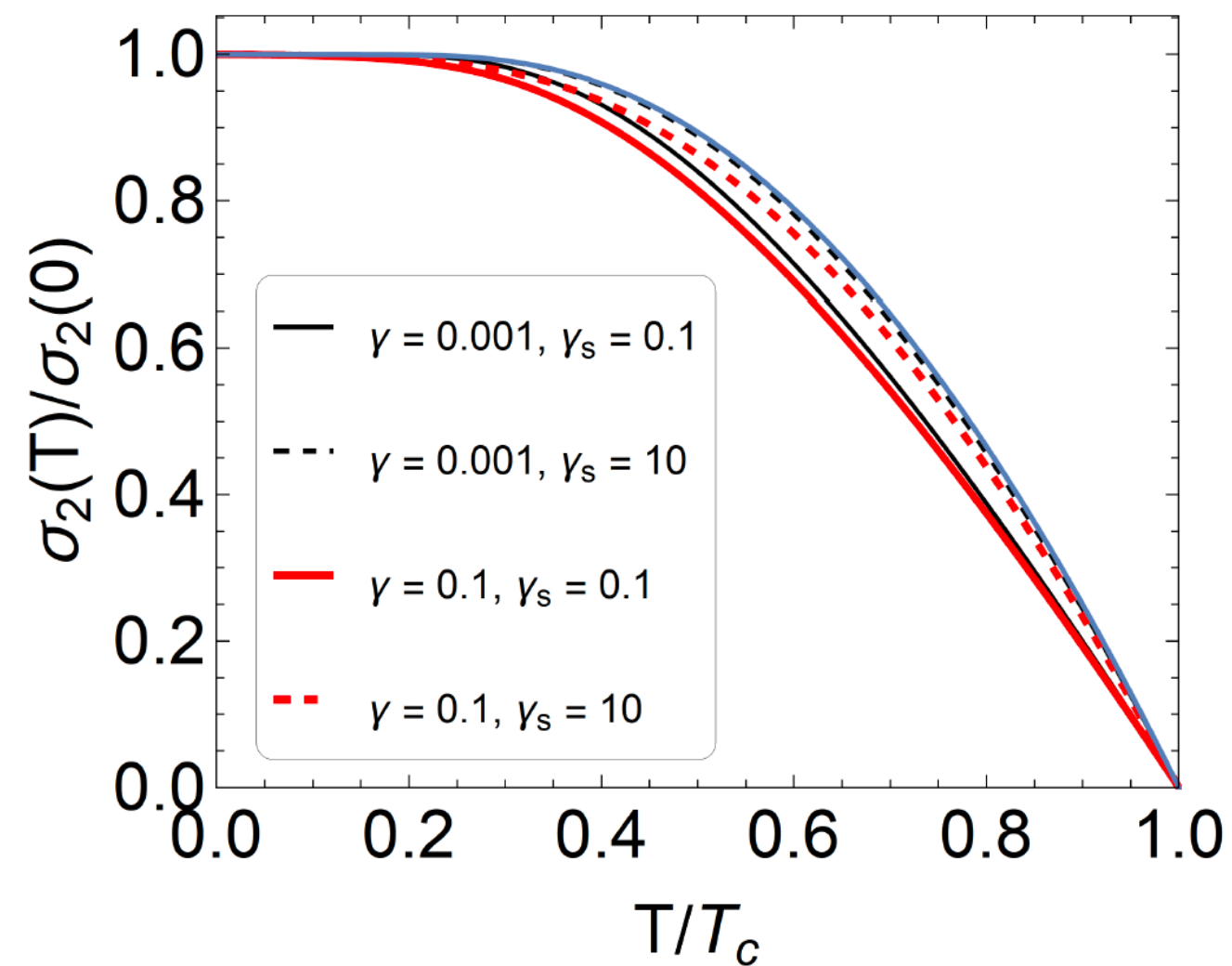


FIG. 6. Temperature dependence of the imaginary part of the microwave conductivity $\sigma_2(T)/\sigma_2(0)$ for several choices of γ and γ_s . Note that when γ_s decreases and γ increases, the curves are pushed slightly downwards with respect to Eq. (14), which is shown by the blue line.

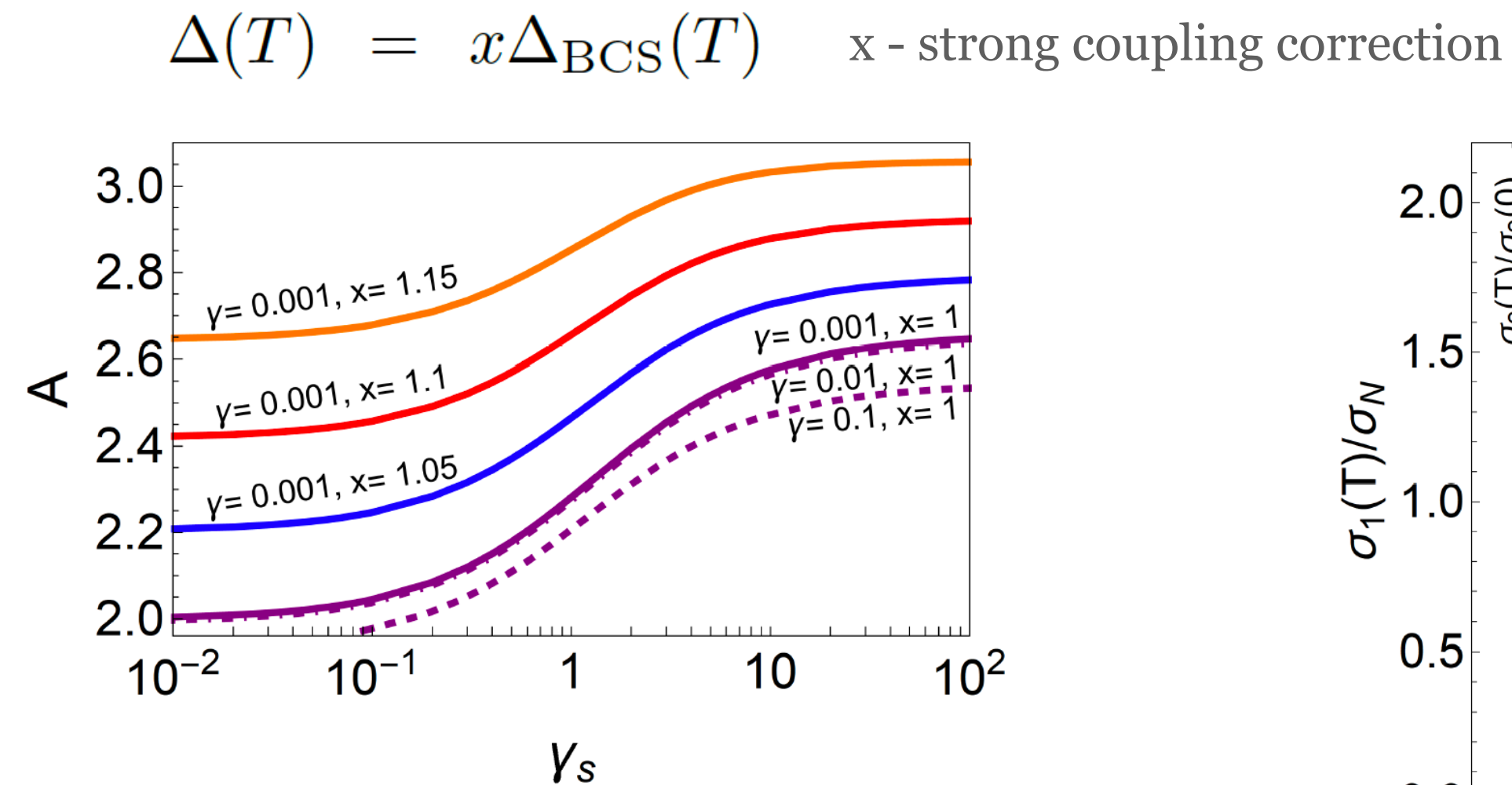


FIG. 7. Coefficient A describing the T -dependence of the imaginary part of the microwave conductivity close to T_c , $\sigma_2(T)/\sigma_2(0) = A(1 - T/T_c)$, plotted as a function of γ_s for several values of γ and x . Note that A depends only very weakly on γ in the limit of small pair breaking.

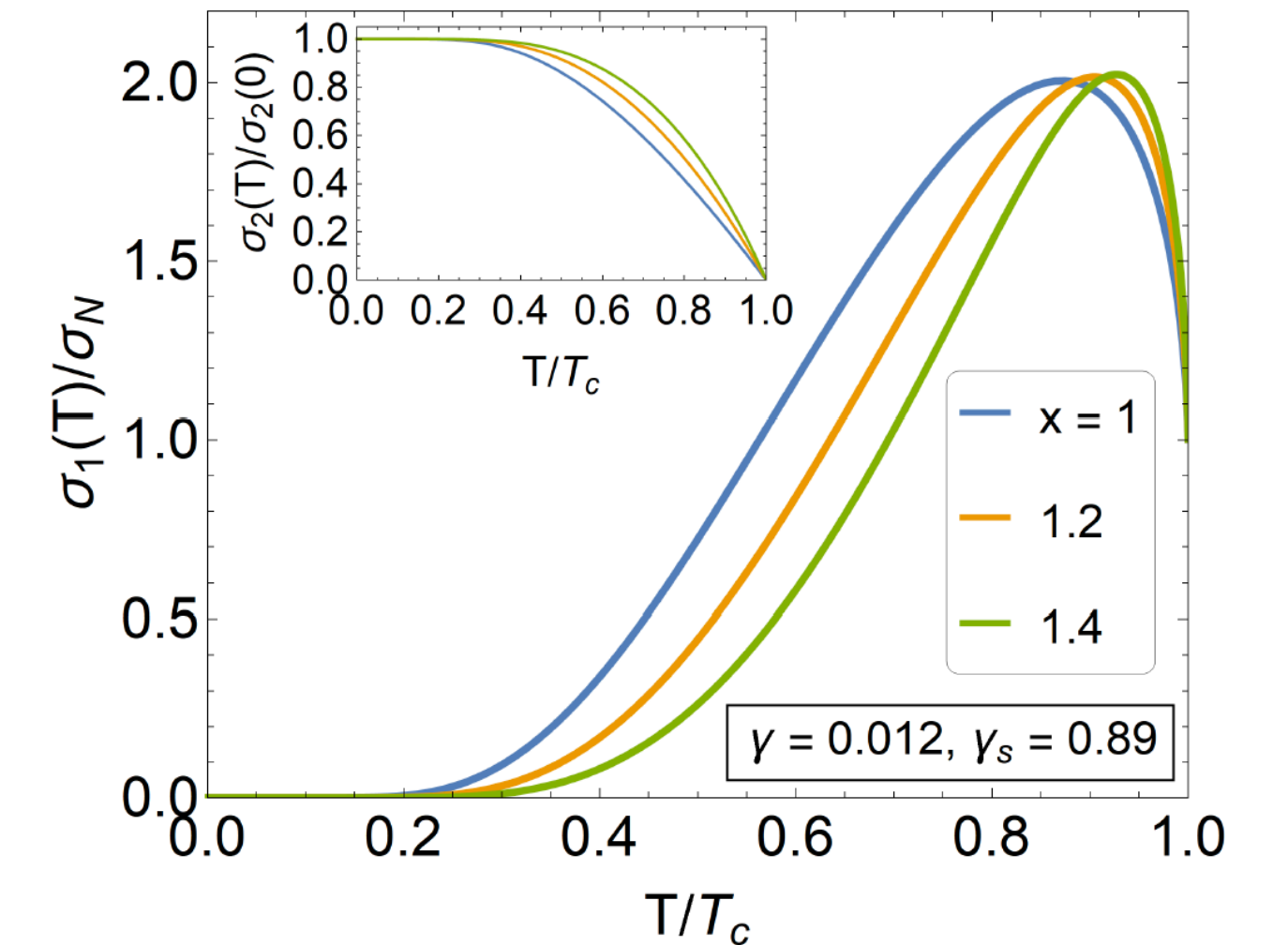


FIG. 8. Evolution of the normalized conductivities $\sigma_1(T)/\sigma_N$ (main panel) and $\sigma_2(T)/\sigma_2(0)$ (inset) with the strong-coupling rescaling parameter x . In both figures we have used $\gamma_s = 0.89$ and $\gamma = 0.012$.



United Nations

Department of Economic and Social Affairs
Sustainable Development

1 NO
POVERTY



2 ZERO
HUNGER



3 GOOD HEALTH
AND WELL-BEING



4 QUALITY
EDUCATION



5 GENDER
EQUALITY



6 CLEAN WATER
AND SANITATION



7 AFFORDABLE AND
CLEAN ENERGY



8 DECENT WORK AND
ECONOMIC GROWTH



9 INDUSTRY, INNOVATION
AND INFRASTRUCTURE



10 REDUCED
INEQUALITIES



11 SUSTAINABLE CITIES
AND COMMUNITIES



12 RESPONSIBLE
CONSUMPTION
AND PRODUCTION



13 CLIMATE
ACTION



14 LIFE BELOW
WATER



15 LIFE
ON LAND



16 PEACE AND JUSTICE
STRONG INSTITUTIONS




17 PARTNERSHIPS
FOR THE GOALS



Research going in similar direction

If not the same

 Cornell University

the Sir

arXiv.org > cond-mat > arXiv:2110.00573

Search...

Help | Adv

Condensed Matter > Superconductivity

[Submitted on 1 Oct 2021]

Effects of nonmagnetic impurities and subgap states on the kinetic inductance, complex conductivity, quality factor and depairing current density

Takayuki Kubo

We investigate how a combination of a nonmagnetic-impurity scattering rate γ and finite subgap states parametrized by Dynes Γ affects various physical quantities relevant to superconducting devices: kinetic inductance L_k , complex conductivity σ , surface resistance R_s , quality factor Q , and depairing current density J_d . All the calculations are based on the Eilenberger formalism of the BCS theory. We assume the device materials are extreme type-II s -wave superconductors. It is well known that the optimum impurity concentration ($\gamma/\Delta_0 \sim 1$) minimizes R_s . Here, Δ_0 is the pair potential for the idealized ($\Gamma \rightarrow 0$) superconductor for the temperature $T \rightarrow 0$. We find the optimum Γ can also reduce R_s by one order of magnitude for a clean superconductor ($\gamma/\Delta_0 < 1$) and a few tens % for a dirty superconductor ($\gamma/\Delta_0 > 1$). Also, we find a nearly-ideal ($\Gamma/\Delta_0 \ll 1$) clean-limit superconductor exhibits a frequency-independent R_s for a broad range of frequency ω , which can significantly improve Q of a very compact cavity with a few tens of GHz frequency. As Γ or γ increases, the plateau disappears, and R_s obeys the ω^2 dependence. The subgap-state-induced residual surface resistance R_{res} is also studied, which can be detected by an SRF-grade high- Q 3D resonator. We calculate $L_k(\gamma, \Gamma, T)$ and $J_d(\gamma, \Gamma, T)$, which are monotonic increasing and decreasing functions of (γ, Γ, T) , respectively. Measurements of (γ, Γ) of device materials can give helpful information on engineering (γ, Γ) via materials processing, by which it would be possible to improve Q , engineer L_k , and ameliorate J_d .

Comments: 15 pages, 15 figures

Subjects: **Superconductivity (cond-mat.supr-con)**; Instrumentation and Methods for Astrophysics (astro-ph.IM); Accelerator Physics (physics.acc-ph)

Cite as: [arXiv:2110.00573](https://arxiv.org/abs/2110.00573) [cond-mat.supr-con]
(or [arXiv:2110.00573v1](https://arxiv.org/abs/2110.00573v1) [cond-mat.supr-con] for this version)

Effects of nonmagnetic impurities and subgap states on the kinetic inductance, complex conductivity, quality factor and depairing current density (Kubo, 2021)

- Kinetic inductance

$$\sigma = \frac{ne^2\tau}{m(1+i\omega\tau)} = \frac{ne^2\tau}{m(1+\omega^2\tau^2)} - i\frac{ne^2\omega\tau^2}{m(1+\omega^2\tau^2)}$$

- Superconductor

$$\frac{1}{2}(2m_e v_s^2)(n_s l A) = \frac{1}{2}L_k I^2$$

$$I = 2ev_s n_s A$$

- Important for kinetic inductance detectors (KIDs) and superconductor single-photon detectors (SSPDs)

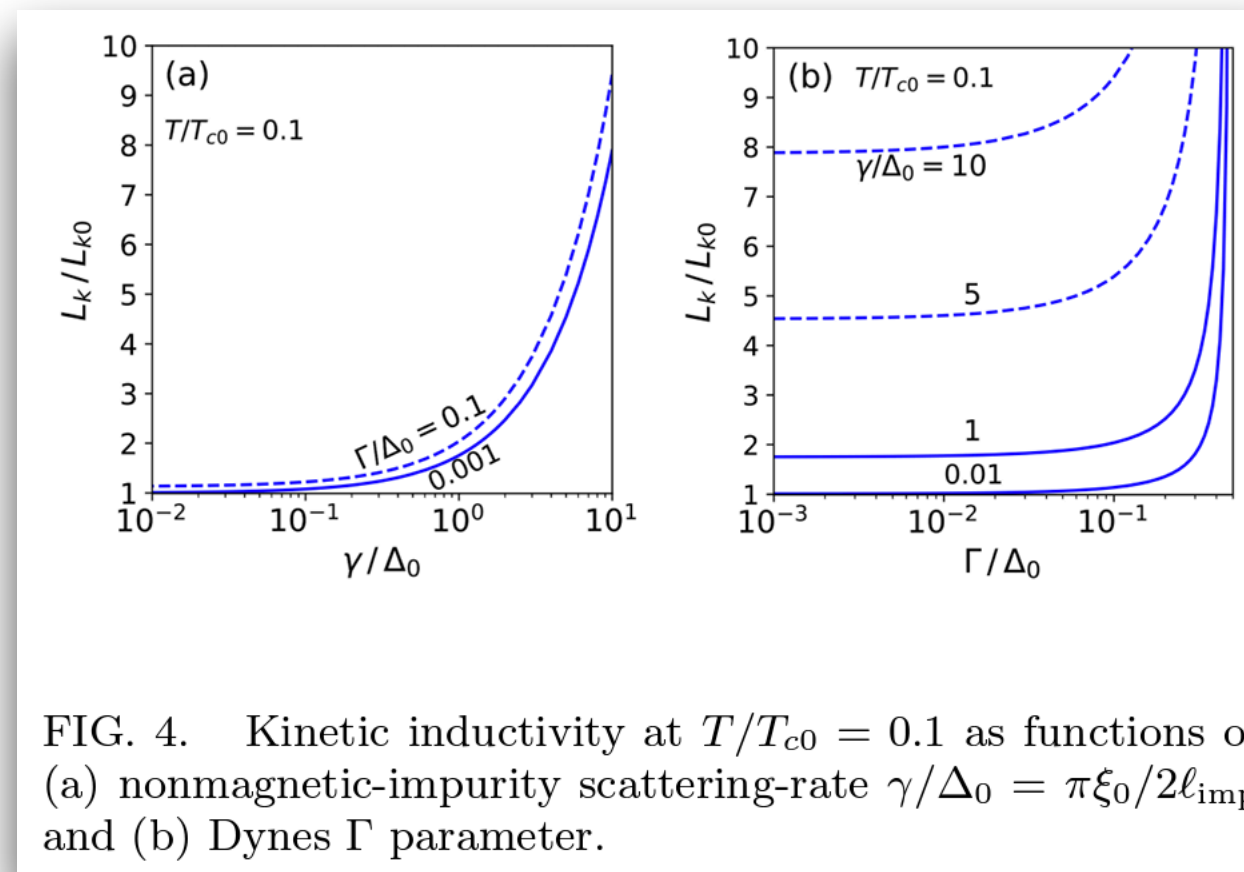


FIG. 4. Kinetic inductivity at $T/T_{c0} = 0.1$ as functions of (a) nonmagnetic-impurity scattering-rate $\gamma/\Delta_0 = \pi\xi_0/2\ell_{\text{imp}}$ and (b) Dynes Γ parameter.

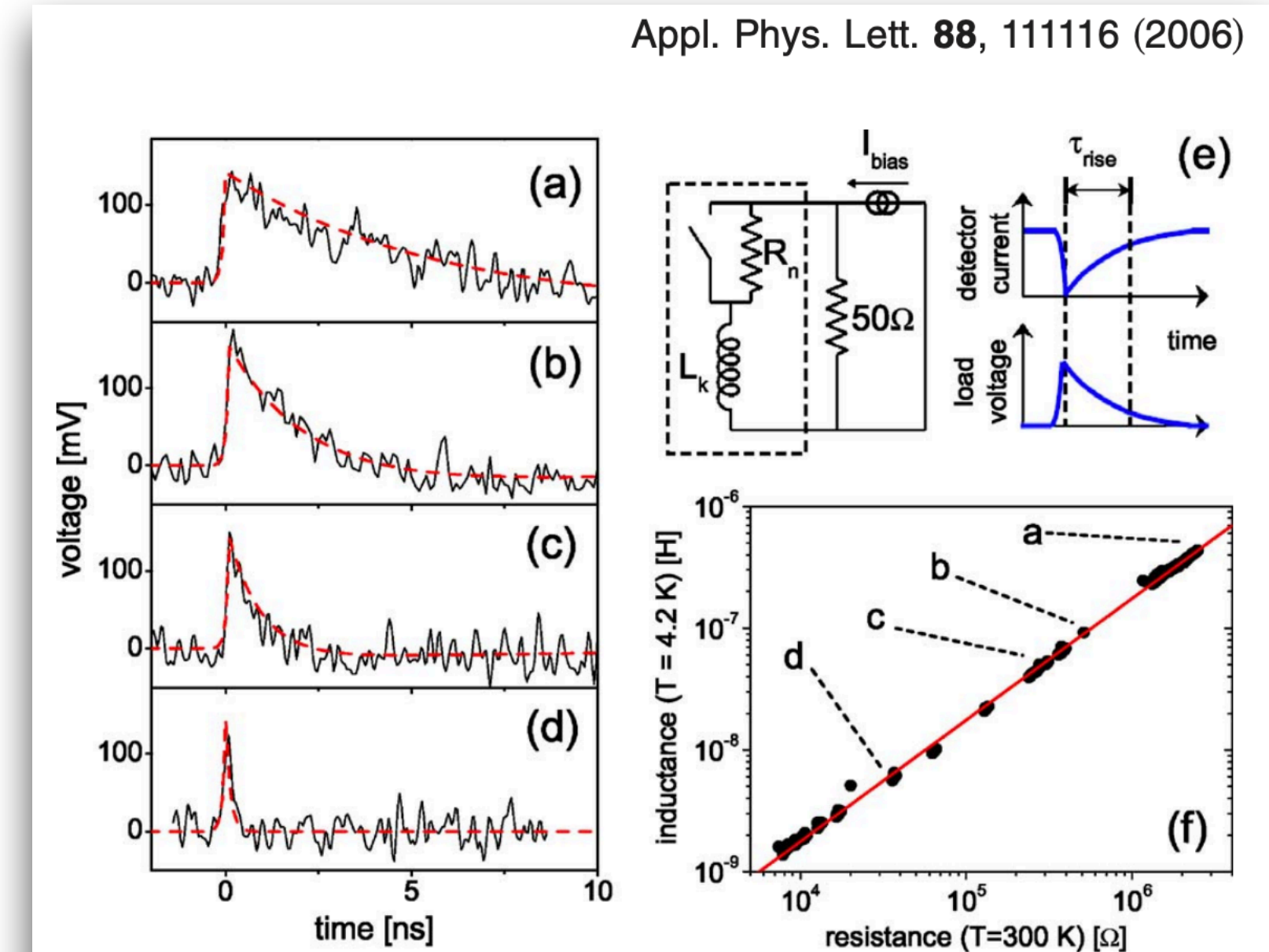


FIG. 2. (Color online) Inductance-limited recovery of NbN nanowires. Output pulses are shown for 100 nm wide wires at $T=4.2$ K, with $I_{\text{bias}}=11.5 \mu\text{A}$, and dimensions: (a) 10 $\mu\text{m} \times 10 \mu\text{m}$ meander (total length 500 μm); (b) 4 $\mu\text{m} \times 6 \mu\text{m}$ (120 μm); (c) 3 $\mu\text{m} \times 3.3 \mu\text{m}$ (50 μm); and (d) 5 μm long single wire. Red dotted lines show the predicted pulse recovery, with no free parameters, for each device based on its measured inductance: $L_k=415$ nH, 110 nH, 44.5 nH, and 6.10 nH. These predictions include the effect of the measured $f_L=15$ MHz and $f_H=4$ GHz corner frequencies of our amplifiers, and the assumptions: $I_{\text{ret}} \ll I_{\text{bias}}$, $R_n \gg 2\pi f_H L_k$, and $R_n \gg 50 \Omega$ (the pulse risetime is then determined by f_H); and (e) electrical model; photon absorption corresponds to the switch opening, after which the detector current goes nearly to zero, and is diverted into the 50 Ω load. The wire then becomes superconducting again, and the current resets in a time τ_{rise} . (f) Inductance at $T=4.2$ K vs room-temperature resistance for 290 individual nanowires from 0.5–500 μm long and 20–400 nm wide, with both straight and meander geometries, from two separate samples made in separate fabrication runs. Points corresponding to the devices of (a)–(d)

Effects of nonmagnetic impurities and subgap states on the kinetic inductance, complex conductivity, quality factor and depairing current density (Kubo, 2021)

- Surface resistance

$$R_s = \frac{1}{2} \mu_0^2 \omega^2 \lambda^3 \sigma_1$$

- Quality

$$Q = \frac{G}{R_s}, \quad G = \frac{\mu_0 \omega \int |\mathbf{H}|^2 dV}{\int |\mathbf{H}|^2 dS}$$

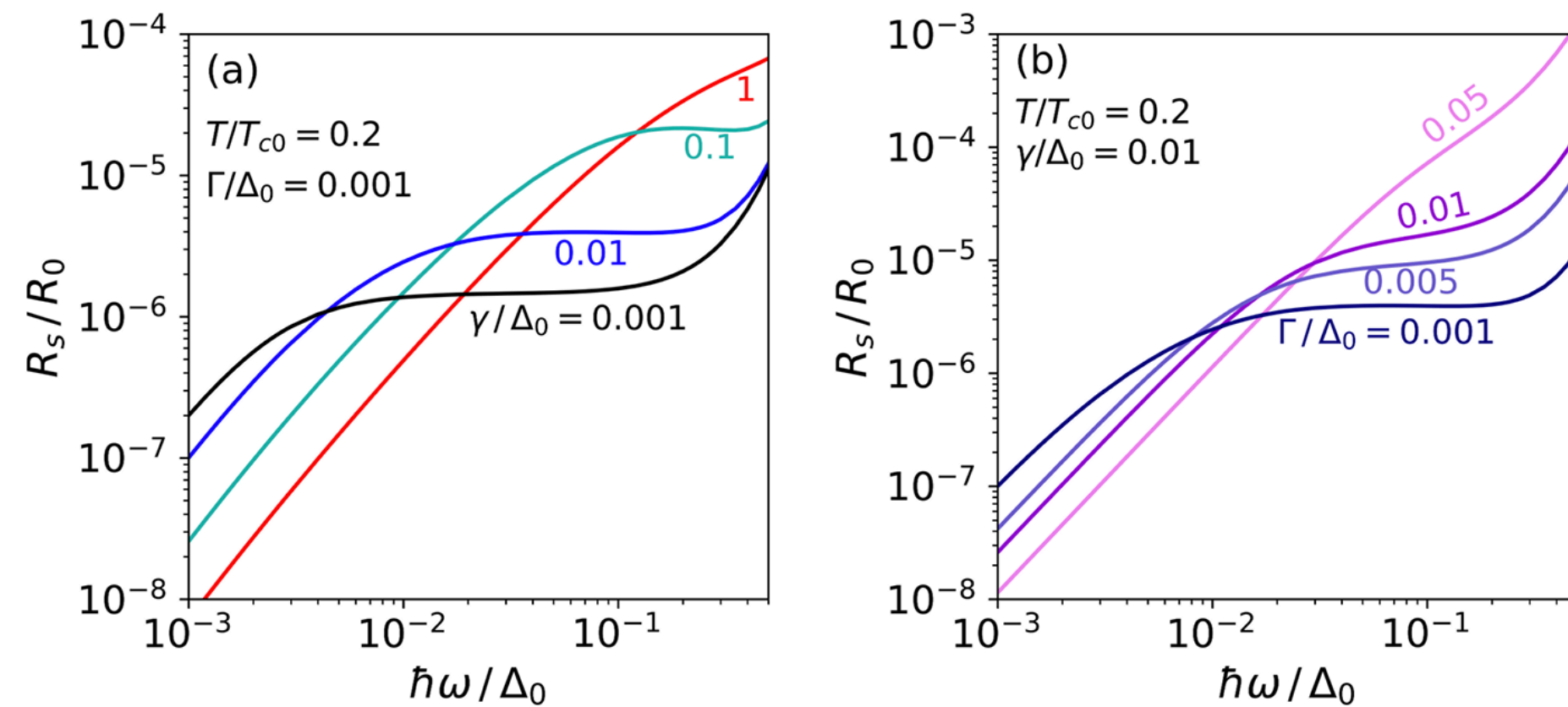


FIG. 10. Frequency dependences of the surface resistance R_s (a) calculated for different nonmagnetic-impurity scattering rate γ and (b) calculated for different Dynes Γ .

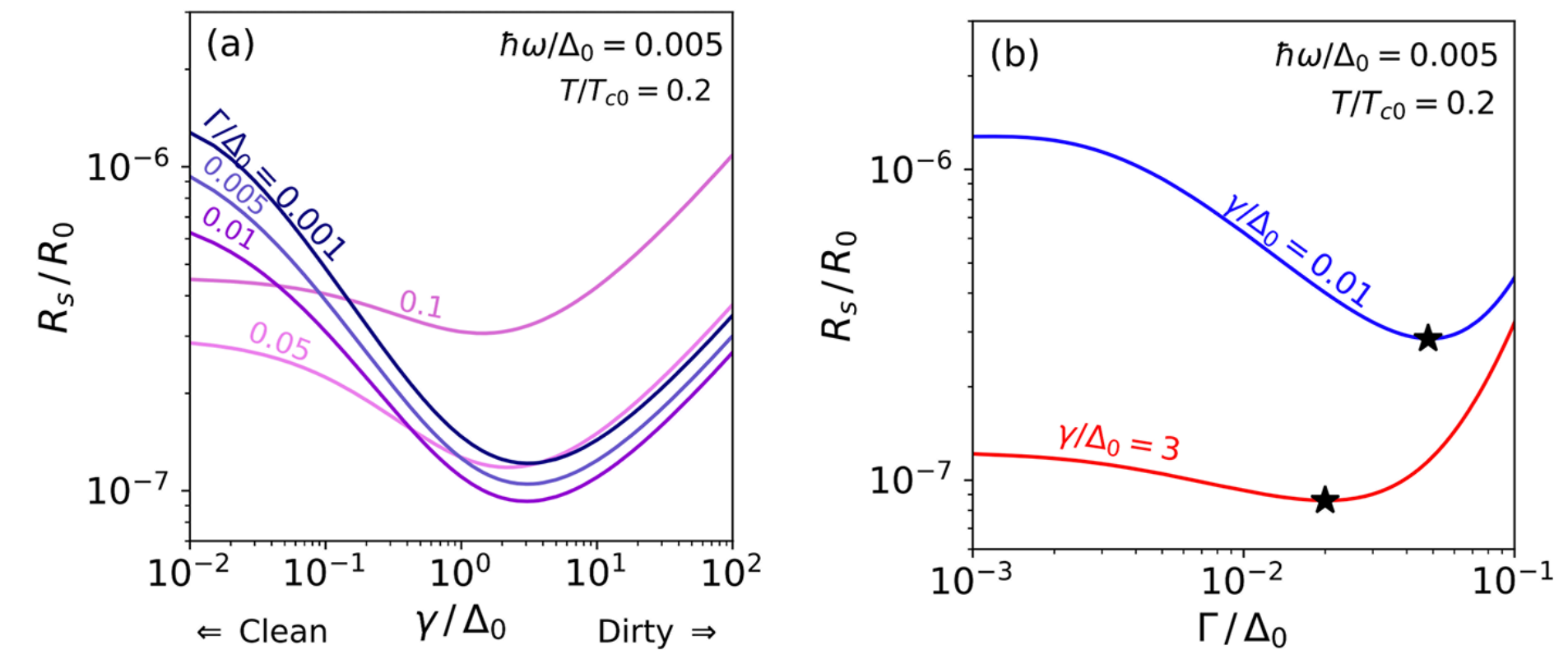


FIG. 11. (a) R_s as functions of nonmagnetic-impurity scattering-rate $\gamma/\Delta_0 = \pi\xi_0/2\ell_{\text{imp}}$ calculated for different Γ . (b) R_s as functions of Γ calculated for $\gamma/\Delta_0 = 3$ (red) and $\gamma/\Delta_0 = 0.01$ (blue). The black stars are the minimums.

Condensed Matter > Superconductivity

[Submitted on 17 Dec 2021]

Model-independent determination of the gap function of nearly localized superconductors

Dušan Kavický, František Herman, Richard Hlubina

The gap function $\Delta(\omega)$ carries essential information on both, the pairing glue as well as the pair-breaking processes in a superconductor. Unfortunately, in nearly localized superconductors with a non-constant density of states in the normal state, the standard procedure for extraction of $\Delta(\omega)$ cannot be applied. Here, we introduce a model-independent method that makes it possible to extract $\Delta(\omega)$ also in this case. The feasibility of the procedure is demonstrated on the tunneling data for the disordered thin films of TiN. We find an unconventional feature of $\Delta(\omega)$ which suggests that the electrons in TiN are coupled to a very soft pair-breaking mode.

- Relation between the densities of states in the normal and superconducting states**

Interesting difference in behaviour of the symmetric and antisymmetric part of the density of states.

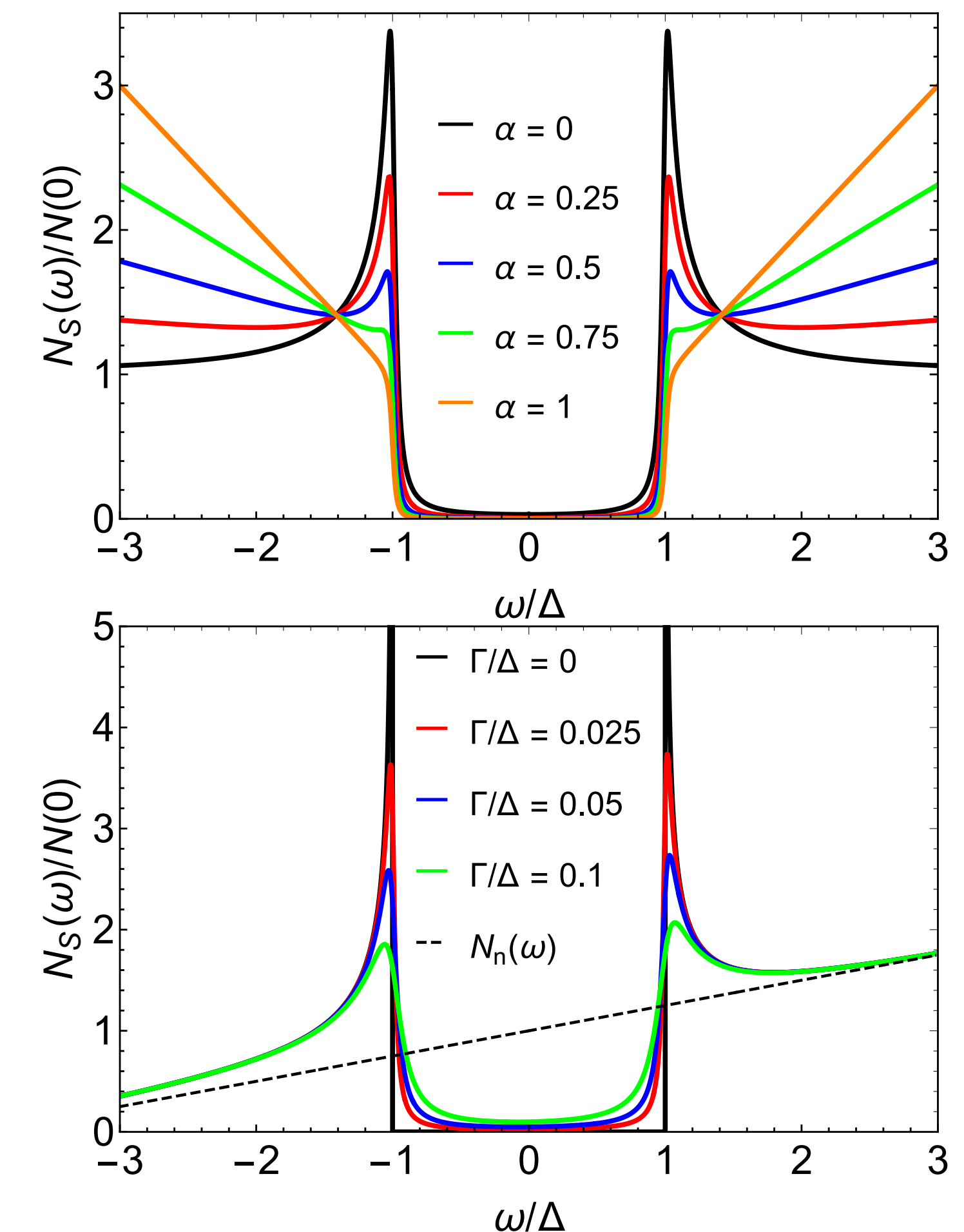
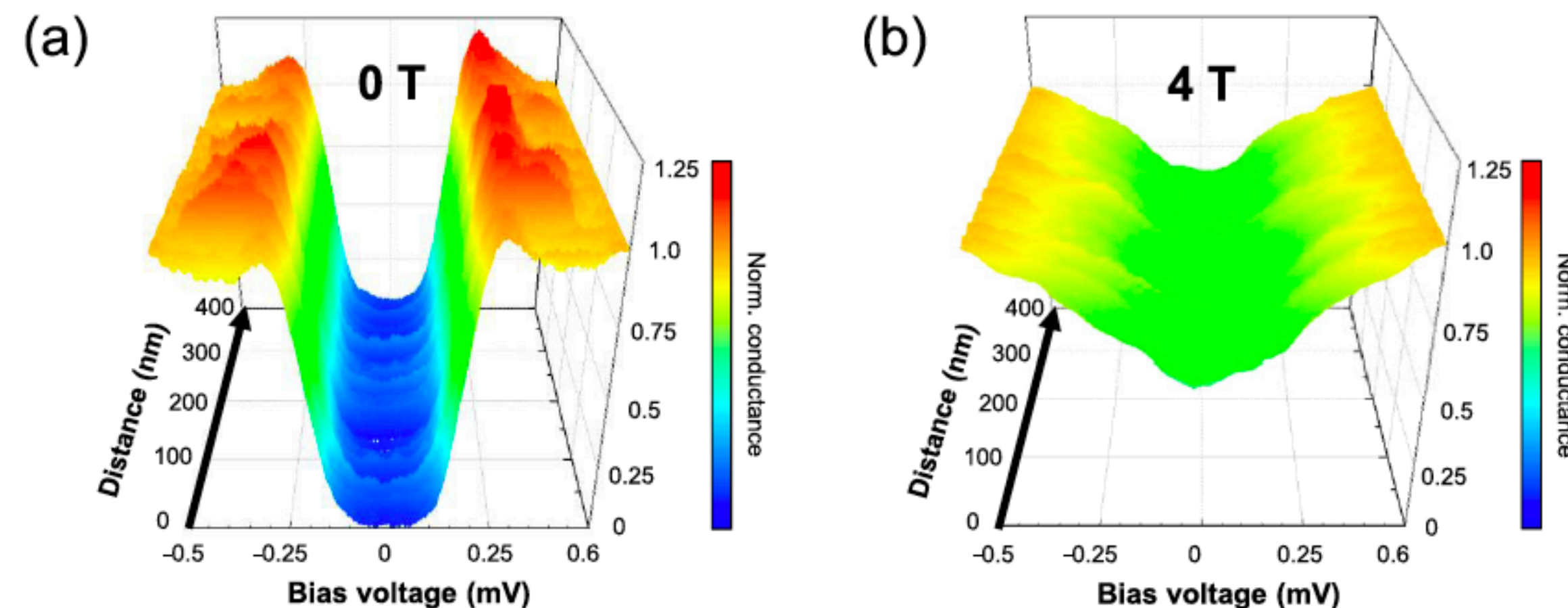
- Reduction of the (quasiparticle) peaks**

Influence of the Pseudogap from the normal state.

- Reduction of the antisymmetry in superconductive region**

- Possible experimental improvement**

Prof. Szabó and Samuely and their group focusing on STM experiment at the SAS in Košice.

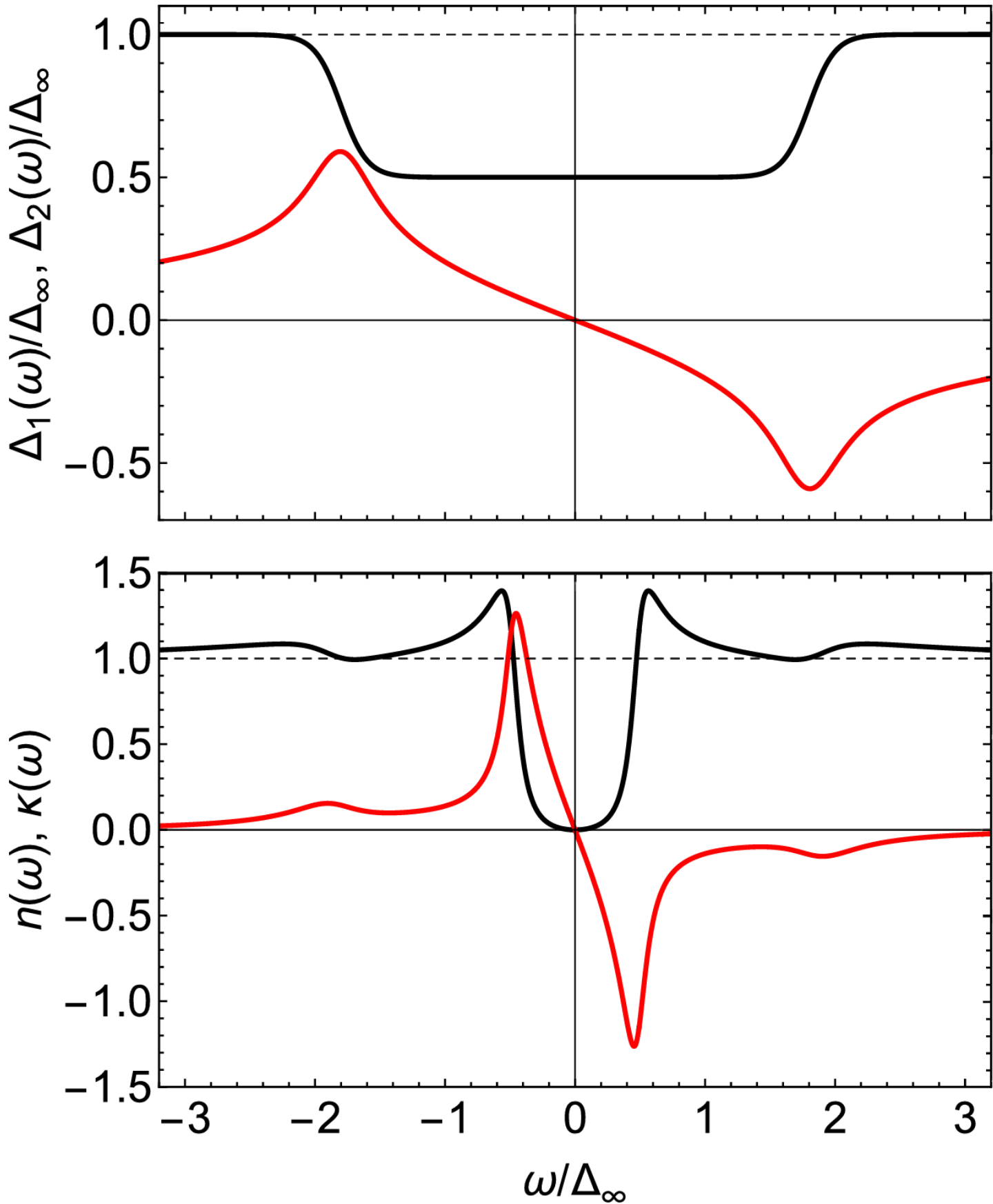
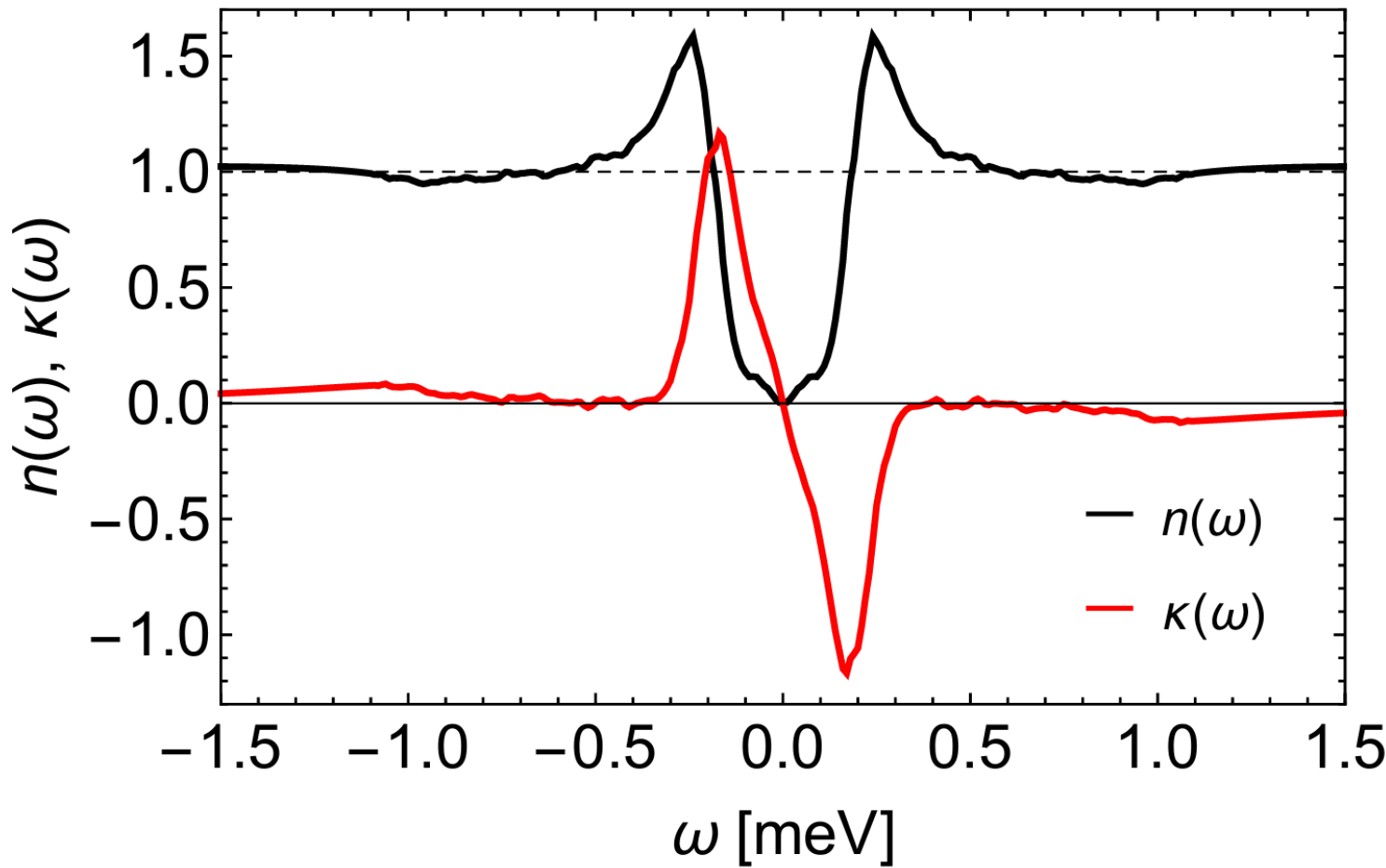


[Submitted on 17 Dec 2021]

Model-independent determination of the gap function of nearly localized superconductors

Dušan Kavický, František Herman, Richard Hlubina

The gap function $\Delta(\omega)$ carries essential information on both, the pairing glue as well as the pair-breaking processes in a superconductor. Unfortunately, in nearly localized superconductors with a non-constant density of states in the normal state, the standard procedure for extraction of $\Delta(\omega)$ cannot be applied. Here, we introduce a model-independent method that makes it possible to extract $\Delta(\omega)$ also in this case. The feasibility of the procedure is demonstrated on the tunneling data for the disordered thin films of TiN. We find an unconventional feature of $\Delta(\omega)$ which suggests that the electrons in TiN are coupled to a very soft pair-breaking mode.



$$\Delta(\omega) = \Delta_\infty + (\Delta_0 - \Delta_\infty) F(\omega),$$
$$F(\omega) = \frac{i}{\pi} \left[\Psi \left(\frac{1}{2} + \frac{\omega + \omega_*}{2\pi i \Theta} \right) - \Psi \left(\frac{1}{2} + \frac{\omega - \omega_*}{2\pi i \Theta} \right) \right]$$

Dynes Superconductors -Implications towards- Radio-Frequency Cavities (František Herman)

Take (stay) home messages

- **Disorder effects reveal characteristic behaviour of the superconductive state.**
- **Understanding the role of the different scattering mechanism can enhance efficiency of the superconducting devices in the current applications.**
- **Model-independent/Theory-model-tested approximative approach may be very powerful tool in the situations where we touch the unknown phenomena, but one needs to be very careful.**

Publications Related to the Dynes superconductivity

- D. Kavický, F. Herman and R. Hlubina, arXiv:2112.09731 (2021),
Model-independent determination of the gap function of nearly localized superconductors,
- F. Herman and R. Hlubina, Phys. Rev. B **104**, 094519 (2021),
Microwave response of superconductors that obey local electrodynamics,
- F. Herman and R. Hlubina, Phys. Rev. B **97**, 014517 (2018),
Thermodynamic properties of the DS,
- F. Herman and R. Hlubina, Phys. Rev. B **96**, 014509 (2017),
Electromagnetic properties of impure superconductors with pair-breaking processes,
- F. Herman and R. Hlubina, Phys. Rev. B **95**, 094514 (2017),
Consistent two-lifetime model for spectral functions of superconductors,
- F. Herman and R. Hlubina, Phys. Rev. B **94**, 144508 (2016),
Microscopic interpretation of the Dynes formula for the tunnelling density of states